

# Interdependencies and causalities in coupled financial networks

Irena Vodenska\*, Hideaki Aoyama, Yoshi Fujiwara,  
Hiroshi Iyetomi, Yuta Arai, H. Eugene Stanley †

version: February 25, 2015

## Abstract

We explore foreign exchange and stock market networks in 48 countries from 1999 until 2012 and propose a model, based on complex principal component analysis, for extracting significant lead-lag relations between these networks, by constructing currency-equity synchronization network. In addition to the analysis for the whole period, we divide the total time period into “mild crisis,” (1999-2002), “calm,” (2003-2006) and “severe crisis” (2007-2012) periods and find that the severe crisis period behavior dominates the dynamics in the foreign exchange-equity interdependent network. We observe that in general the foreign exchange market has predictive power for the global stock market performance. Also, the United States, German and Canadian markets have forecasting power for the performances of other global equity markets.

Key words: Complex Principal Component Analysis, Interdependent Networks, Financial Crisis, Foreign Exchange  
JEL classification: F31, G01, G15

---

\*Corresponding author, Email: vodenska@bu.edu

†Vodenska is with Boston University Metropolitan College (finance) and Center for Polymer Studies. Aoyama is with Kyoto University Physics Department. Fujiwara is with the University of Hyogo Graduate School of Simulation Studies. Iyetomi and Arai are with Niigata University Graduate School of Science and Technology. Stanley is with Boston University Department of Physics and Center for Polymer Studies. We are extremely grateful to Y. Ikeda, H. Souma, and H. Yoshikawa for helpful discussions and comments that greatly improved the paper. In addition, the authors thank Boston University School of Management for providing Bloomberg pricing data. This work is partially supported by Grant-in-Aid for Scientific Research (KAKENHI) Grant Numbers 25282094 and 25400393 by JSPS, the Program for Promoting Methodological Innovation in Humanities and Social Sciences by Cross-Disciplinary Fusing of the JSPS, and the European Community Seventh Framework Programme (FP7/2007-2013) under Socio-economic Sciences and Humanities, grant agreement no. 255987 (FOC-II) and 297149 (FOC-INCO).

## I. Introduction

OUR DAILY LIVES are strongly affected by various complex systems such as communication, financial transactions, transportation, just to name a few. The development of modern societies relies on the proper functioning and reliability of these underlying infrastructures. The real world does not function as a set of independent systems but rather of many interdependent systems that interact with each other. Needless to say, our world is becoming more interconnected and any progress or development in one part of the world can be seamlessly exported to another.

Complexity science has been utilized for analyses of interconnectedness in various systems concerning our global world, not the least of which is the international financial and economic complex system. Interdependent network studies (Buldyrev et al. (2011), Gao et al. (2011)) have found that coupled networks are more vulnerable to shocks in the system than single isolated networks, and that damage propagates more rapidly in coupled networks than in isolated networks. Thus adverse effects in a coupled system are more severe than in an isolated system.

A large body of literature studying stock markets and currency markets from various perspectives has emerged as financial markets have changed and cross-border capital flow has increased. The majority of the capital flow increase has been in form of equity investments, with a much smaller portion allocated to overseas loans and fixed income investments. For example, Gagnon and Karolyi (2006) report that the total gross capital flows (gross capital purchases and sales between U.S. and foreign investors of U.S. and foreign assets) have increased from less than \$100 billion in 1977, corresponding to 1% of U.S. Gross Domestic Product, to over \$3.5 trillion, or approximately 30% of U.S. GDP. This significant increase in foreign equity purchases and sales indicates the importance of understanding the relationship between stock markets and foreign exchange markets. Previous studies have investigated the comovements and dependency structures between stock markets and foreign exchange rates (Dornbusch and Fischer (1980), Dooley and Isard (1982), Granger et al. (2000), Morley (2002), Nieh and Lee (2002), Bae et al. (2003), Cappiello and De Santis (2005), Gagnon and Karolyi (2006) Pan et al. (2007), Ning (2010), Zhao (2010), Katechos (2011), Lin (2012)).

Bae et al. (2003) study international market returns and foreign exchange changes and propose an approach to evaluate contagion in financial markets based on coincidental return shocks in different countries. They use multinomial logistic regression and find that contagion is predictable and depends on interest rates, exchange rate changes, and conditional stock return volatilities. Gagnon and Karolyi (2006) suggest that the co-movements in international financial markets are a by-product of increased international cross-border capital flow. According to this study, International markets seem to depend more on other international markets than on country's domestic fundamentals.

Other studies have focused on stock return predictability in the United States (Fama and French (1988, 1989), Breen et al. (1989), Cochrane (2008)) and globally (e.g. Harvey (1991), Bekaert and Hodrick (1992), Ferson and Harvey (1993), Patro

and Wu (2004), Rapach and Wohar (2006), Ang and Bekaert (2007), Hong et al. (2007), Cohen and Frazzini (2008), Welch and Goyal (2008), Bekaert et al. (2009), Hjalmarsson (2010), Menzly and Ozbas (2010), Ferreira and Santa-Clara (2011), Bollerslev et al. (2012), Rapach et al. (2013), Dahlquist and Hasseltoft (2013)) reporting mixed results, finding positive or negative correlations, stable or non-stable causality relations between markets, and regional and temporal diversity.

Rapach et al. (2013) found that lagged U.S. market returns have been powerful predictor of returns for many other industrialized countries, forecasting returns better than these countries' economic indicators shedding new light on international predictability. This study uses predictive regression models, pairwise Granger causality tests, and an empirical news diffusion model to analyze how return shocks in one country affect returns in another country. Finally, they also examine the out-of-sample predictive power of lagged U.S. returns and find that out-of-sample gains for numerous non-U.S. countries tend to concentrate during business cycle recessions. These gains have been particularly strong during the most recent Global Financial Crisis (GFC).

The GFC, considered by many to be the worst crisis since the great depression of the 1930s, threatened major financial institutions with the possibility of systemic collapse, propagated value deterioration to financial markets around the world, and involved national governments in bailing out systemically important financial institutions. The crisis also adversely affected housing markets and real estate prices globally and contributed to increased unemployment rates and prolonged workforce unemployment. Ultimately, the global financial meltdown contributed to the European sovereign debt crisis with consequences still lingering in the global financial system. The increased interconnectedness of the financial system up to a certain level could bring stability to the system; however, above a critical point, the system could rapidly become extremely vulnerable, prone to a first-order-like abrupt phase transition (Acemoglu et al. (2013), Huang et al. (2013), Dehmamy et al. (2014))

Using a network science approach to study the dynamics of financial and economic systems reveals important relationships and defining characteristics within real-world influences that may be overlooked by approaches that do not take into consideration the relationships among the connected parts of the complex financial system. Previous studies related to financial systems (Billio et al. (2010), Gai et al. (2011), Huang et al. (2011), Haldane and May (2011), Battiston et al. (2012), Aoyama et al. (2013), Huang et al. (2013)) have shed light not only on the topology of financial networks, i.e., the monetary and information flow within economic and governance networks, but have also examined systemic risk propagation. Acemoglu et al. (2012) argue that macroeconomic shocks that originate in one sector may not necessarily be contained close to the origin, but rather could spill over to other parts of the economy affecting other sectors' outputs generating significant aggregate effect. This study illuminates the often ignored cascading failure effect that could contribute to disastrous consequences in the entire economic system.

The objective of this paper is to study the complex interdependencies and their increasingly interrelated nature of the coupled *global* economic and financial net-

works, by the use of the latest concepts and methodology from statistical physics and complexity science, to reveal the intrinsic relations in interacting networks. Understanding the interconnectedness and lead-lag relations in the economic complex system could be useful for forecasting the effect of one part of the system on another and potentially offering efficient strategies for system recovery (Majdandzic et al. (2015)).

Unlike previous studies, which have focused on relatively small groups of countries—e.g., G-5, G-7, or the emerging Asian countries, we examine a truly global set of 48 countries, including large and small countries in Europe, the Americas, Asia, and the Middle East. Although we find aspects of regional domination in some local economic communities, using a non-trivial global analysis we also find that these local “economic regions” display network characteristics that are shaped by forces that extend far beyond the local “geographic regions” explored in previous research. The value of our study lies in its use of a novel methodology based on a Complex Principal Component Analysis (CPCA) applied to a broad range of economic networks that encompasses more than one world region and more than one characteristic time period.

More specifically, we present a new approach to study the causal relationships between stock and foreign exchange markets. The cross-market relationships that we investigate have significant implications for international risk management and global portfolio management. Understanding the dynamics of the relationship between currency and stock markets is also essential for policy makers. For instance if most of the spillover effects between stock and currency markets are caused by stock market shocks that transfer into currency markets, the policy implications of this phenomenon suggest that a focus on stock-market-centered stability policies might help prevent currency crises. If however shocks propagate from currency to stock markets stabilizing policies for currencies might prove useful in halting or localizing stock market crashes.

In building our analysis we use the CPCA approach, utilizing the Hilbert transformation and the Rotational Random Shuffling (RRS) methods to identify true comovements, free from contamination of noises, to study the lead-lag relationships between foreign exchange and equity market returns. Our paper offers three methodological advantages over the previous studies: (i) CPCA enables us to detect beyond-pairwise lead-lag relations as compared with the traditional Granger causality and cross-correlation analysis; (ii) CPCA is able to extract dynamical correlations simultaneously, while this is difficult to accomplish with PCA; and (iii) RRS provides us with a sound null hypothesis to identify statistically meaningful correlations.

The rest of this paper is organized as follows: In section II we describe the data and the methodology, namely, CPCA and RRS. In section III we present the results obtained by the analysis of dominant and significant eigenmodes. In addition to identifying and analyzing the three largest eigenvalues, we also take into account the importance of smaller but still significant eigenvalues that shed light on the effect of important global economic developments. In section IV we analyze the community structure of the currency-equity synchronization network and explore the lead-lag

relationships between communities. We obtain stable lead-lag relationships for the majority of the network communities with one community emerging as an exception. In section V we discuss our results and offer concluding remarks.

## II. Data and Methodology

We study daily pricing data for foreign exchange quotes and major stock market indices for 48 countries (see Table 1) for the 14-year period from Jan. 1, 1999 to Dec. 31, 2012 (5,114 calendar days with 3,652 trading days). We obtain the data from Boston University’s Bloomberg database, which provides financial data for use in academic research.

The time-designation “day” will differ in different parts of the world because of differences in world time zones. Weekends are also missing from the data. However, our methodology is suitable for overcoming these issues, as we discuss later in this section.

We denote this data as  $S_\alpha(t)$ , where the node index  $\alpha = 1, 2, \dots, 48$  are the stock-market indices of the 48 countries,  $\alpha = 49, \dots, 96 (= N)$  the currencies of the 48 countries in the same order as in Table. 1, and  $t = 1, 2, \dots, 3652$  the date-numbers. The time series we analyze are the log-returns (the logarithm of the growth-rate)  $r_\alpha(t)$  defined by

$$r_\alpha(t) := \log_{10} \left[ \frac{S_\alpha(t+1)}{S_\alpha(t)} \right] \times \begin{cases} +1 & \text{for } 1 \leq \alpha \leq 48 \\ -1 & \text{for } 49 \leq \alpha \leq 96 \end{cases} \quad (1)$$

where  $t$  runs from 1 to 3651 ( $\equiv T$ ).

































































































The currency quotes that we analyze are expressed as currency/SDR.<sup>1</sup> So when the price thus expressed increases, it means that the currency has depreciated and more “currency” is needed for one SDR. For example, if the USD/SDR price increases, this means that the US Dollar has depreciated.

To avoid confusion and to allow a comparison between the increases (or decreases) in stock market values and the appreciation (or depreciation) of currencies, we transform our original data series from currency/SDR into SDR/currency by multiplying the currency log-returns by  $(-1)$ .

---

<sup>1</sup>Special drawing right (SDR) is defined as a basket of four major currencies (Japanese Yen, US Dollar, Pound Sterling, and the Euro). The composition of the SDR basket is reviewed every five years by the Executive Board of the International Monetary Fund to ensure that it reflects relative importance of currencies in the global financial and trading systems. The last SDR revision took place in November 2010, and the changes became effective on January 1, 2011. The next SDR review will take place in 2015.

**Table 1: List of 48 countries with their stock-market indices and currencies (with gray hexagonal background).** These markers (symbols) are used in the subsequent figures throughout the paper. For the top ten countries (2012 GDP, less China), the markers are given individually with flag motifs, while for others the markers reflect their regionality.

No.	Country	Stock Index	Currency
1	UK	 UKX	 Pound Sterling
2	Austria	 ATX	 Euro
3	Belgium	 BEL20	 Euro
4	Finland	 HEX25	 Euro
5	France	 CAC	 Euro
6	Germany	 DAX	 Euro
7	Ireland	 ISEQ	 Euro
8	Italy	 FTSEMIB	 Euro
9	Netherlands	 AEX	 Euro
10	Portugal	 PSI20	 Euro
11	Spain	 IBEX	 Euro
12	Greece	 ASE	 Drachma, then Euro since Jan. 2001
13	Malta	 MALTEX	 Maltese Lira, then Euro since Jan. 2008
14	Slovakia	 SKSM	 Slovak Koruna, then Euro since Jan. 2009
15	Norway	 OBX	 Norwegian Krone
16	Sweden	 OMX	 Swedish Krona
17	Iceland	 ICEXI	 Icelandic Krona
18	Switzerland	 SMI	 Swiss Franc
19	Czech	 PX	 Czech Koruna
20	Denmark	 KFX	 Danish Krone
21	Hungary	 BUX	 Forint
22	Poland	 WIG	 Zloty
23	Russia	 INDEXCF	 Ruble
24	USA	 SPX	 US Dollar
25	Canada	 SPTSX	 Canadian Dollar
26	Mexico	 MEXBOL	 Mexican Peso
27	Brazil	 IBOV	 Real
28	Argentina	 Merval	 Argentine Peso
29	Chile	 IPSA	 Chilean Peso
30	Peru	 IGBVL	 Nuevo Sol
31	Venezuela	 IBVC	 Bolivar
32	India	 SENSEX	 Indian Rupee
33	Sri Lanka	 CSEALL	 Sri Lankan Rupee
34	Indonesia	 JCI	 Indonesian Rupiah
35	Japan	 NKY	 Yen
36	South Korea	 KOSPI	 South Korean Won
37	Malaysia	 FBMKLCI	 Ringgit
38	Thailand	 SET	 Baht
39	Philippine	 PCOMP	 Philippine Peso
40	Hong Kong	 HSI	 Hong Kong Dollar
41	Australia	 AS51	 Australian Dollar
42	Israel	 TA-25	 Shekel
43	Pakistan	 KSE100	 Pakistani Rupee
44	Saudi Arabia	 SASEIDX	 Saudi Riyal
45	South Africa	 TOP40	 Rand
46	Oman	 MSM30	 Rial
47	Qatar	 DSM	 Riyal
48	Mauritius	 SEMDEX	 Mauritian Rupee

**Table 2: Summary Statistics for the log-returns.** Here  $\mu$  is the mean in units of  $10^{-5}$ ,  $\sigma$  the standard deviation in units of  $10^{-3}$ ,  $\gamma_1$  the skewness (the third standardized moment), and  $\beta_2$  the kurtosis (the fourth standardized moment, equal to three for normal distribution).

No.	Country	Stock Index				Currency			
		$\mu$	$\sigma$	$\gamma_1$	$\beta_2$	$\mu$	$\sigma$	$\gamma_1$	$\beta_2$
1	UK	0.03	5.50	-0.14	8.79	-1.30	2.45	-0.21	5.56
2	Austria	9.06	6.34	-0.31	10.64	0.39	2.70	0.09	4.31
3	Belgium	-4.17	5.73	0.06	8.79	0.39	2.70	0.09	4.31
4	Finland	4.71	7.01	-0.07	5.92	0.39	2.70	0.09	4.31
5	France	-0.95	6.65	0.03	7.66	0.39	2.70	0.09	4.31
6	Germany	4.99	6.89	0.00	7.18	0.39	2.70	0.09	4.31
7	Ireland	-4.59	6.22	-0.56	10.66	0.39	2.70	0.09	4.31
8	Italy	-9.25	6.63	-0.05	7.82	0.39	2.70	0.09	4.31
9	Netherlands	-5.37	6.63	-0.09	8.92	0.39	2.70	0.09	4.31
10	Portugal	-7.91	5.04	-0.14	10.63	0.39	2.70	0.09	4.31
11	Spain	-2.21	6.65	0.11	8.15	0.39	2.70	0.09	4.31
12	Greece	-13.13	7.80	0.03	7.09	-0.07	2.67	0.10	4.37
13	Malta	11.60	3.59	1.35	18.92	0.72	2.65	0.20	18.54
14	Slovakia	8.51	5.45	-1.08	19.05	4.70	2.80	0.13	4.36
15	Norway	16.59	7.05	-0.55	9.33	2.65	3.23	-0.13	6.17
16	Sweden	5.41	6.95	0.07	6.10	1.60	3.32	0.02	5.34
17	Iceland	-5.16	9.10	-37.38	1838.72	-8.31	4.32	0.54	65.35
18	Switzerland	-0.58	5.32	-0.03	9.24	3.80	3.00	-0.52	11.96
19	Czech	11.52	6.45	-0.44	14.70	4.44	3.38	0.05	5.45
20	Denmark	9.71	5.66	-0.22	8.61	0.41	2.70	0.09	4.31
21	Hungary	12.59	7.16	-0.04	8.94	-1.34	3.97	-0.39	7.37
22	Poland	14.04	5.97	-0.36	6.62	0.44	3.81	-0.15	7.14
23	Russia	41.42	10.45	-0.03	13.82	-5.72	2.43	-1.31	38.95
24	USA	1.77	5.70	-0.15	10.48	-1.04	1.34	-0.08	6.04
25	Canada	7.74	5.16	-0.64	11.67	4.15	2.69	-0.12	4.97
26	Mexico	28.56	6.26	0.10	7.32	-4.14	3.14	-0.64	11.72
27	Brazil	26.12	8.46	0.76	19.30	-7.34	4.97	-0.23	14.26
28	Argentina	22.51	9.06	-0.08	8.52	-19.98	4.11	-14.14	468.30
29	Chile	20.21	4.55	0.08	11.70	-1.18	2.87	-0.18	6.08
30	Peru	32.56	6.19	-0.52	14.99	1.50	1.74	-0.04	7.56
31	Venezuela	54.59	6.38	-0.29	25.79	-25.18	6.41	-30.25	1420.36
32	India	13.74	6.29	-0.50	9.85	-4.07	1.76	0.32	7.28
33	Sri Lanka	26.71	5.19	0.36	33.00	-8.46	1.92	-2.52	58.49
34	Indonesia	28.35	6.49	-0.36	9.57	-3.18	3.98	0.27	16.24
35	Japan	-3.41	6.52	-0.39	10.17	2.17	2.94	0.03	7.02
36	South Korea	8.24	7.03	-0.49	9.85	0.43	3.20	0.09	27.03
37	Malaysia	12.59	4.14	-0.52	11.95	1.54	1.55	-0.11	6.36
38	Thailand	16.23	6.44	-0.36	12.04	1.01	1.70	-0.12	8.22
39	Philippine	12.88	5.83	0.40	18.48	-1.68	2.16	3.34	75.49
40	Hong Kong	9.67	6.90	-0.05	10.38	-1.05	1.32	-0.05	6.08
41	Australia	6.39	4.41	-0.50	9.16	5.29	3.66	-0.25	12.06
42	Israel	15.84	5.66	-0.26	6.10	0.17	2.19	-0.12	7.86
43	Pakistan	34.31	6.37	-0.25	6.48	-9.03	2.14	-0.10	12.50
44	Saudi Arabia	18.58	6.60	-1.04	13.6	-1.05	1.36	-0.06	5.93
45	South Africa	24.43	5.94	-0.11	6.56	-5.35	4.82	-1.08	16.79
46	Oman	10.69	4.36	-0.54	20.96	-1.04	1.39	0.00	6.62
47	Qatar	21.59	7.96	-0.25	23.25	-1.06	1.34	-0.07	6.09
48	Mauritius	15.63	3.67	-0.46	191.26	-3.56	3.72	-0.36	12.03

Table 2 displays an overview of the summary statistics for each country’s stock market performance and currency returns. Note that while Pakistan, Russia, and Venezuela show daily stock market returns of over 0.079%, 0.095%, and 0.12%, respectively, European countries such as Greece, Italy, and Portugal show negative daily stock market returns of over  $-0.03\%$ ,  $-0.02\%$ , and  $-0.018\%$ , respectively, between 1999 and 2012. Almost all of the American, Asian, and the Middle Eastern stock markets show positive returns, with the exception of Japan with a  $-0.008\%$  return. Russia, Iceland, and Argentina show the highest stock market volatilities, while Malta, Malaysia, and Mauritius appear to have the lowest. Iceland exhibits the largest positive skew, significantly different from all the other countries, and the highest kurtosis, followed by Mauritius showing the next highest stock market kurtosis, approximately 10 times lower than Iceland. European and Asian countries show mixed currency returns, while the American and the Middle Eastern countries show primarily negative currency returns. Currencies display lower volatilities than stock markets. Venezuela and Argentina exhibit the largest positive skewness and kurtosis, with the magnitude for Venezuela being approximately three times the magnitude for Argentina for both skewness and kurtosis.

Table 3 displays the summary statistics for periods 1, 2, and 3. In period 2 (2003–2006) we see the highest positive global stock market returns of 0.09–0.13% and a relatively low volatility of 0.01–0.013%. The currency results for the same period are mixed. The stock markets on average are not significantly skewed. The Middle Eastern stock markets show the highest kurtosis in period 2, while the European stock markets exhibit highest kurtosis in period 3. Currencies on average show mixed returns with relatively low volatility. American currencies exhibit positive skewness and significant kurtosis in all 3 periods.

We analyze the co-movements of these time series for both equal-time and possible time-delays by applying CPCA, which consists of the following steps:

- A. We construct a complex time series by adding the Hilbert transform of the time series as the imaginary component.
- B. We do a correlation analysis to obtain the eigenmodes for the period of interest.
- C. We do a rotational random shuffling (RRS) simulation to identify which eigenmodes are significant, i.e., which represent co-movements between time series.

This methodology is suitable for efficiently extracting significant lead-lag relationships among currencies and financial markets. The CPCA efficiently identifies significant lead-lag relationships in the global financial network that occur due to the difference of a “day” in different parts of the world as well as lead-lag relationships due to real time-delay in the reactions of one country to economic phenomena in other countries. Computational efficiency is especially important since we analyze a large dataset consisting of 96 time-series. One may apply ordinary cross-correlation analysis by shifting each time-series and maximizing the correlation coefficients as functions of time-shifts. However, doing so for all the possible



**Table 3: Summary Statistics for the log-returns in each period.** Here  $\mu$  is the mean in units of  $10^{-5}$ ,  $\sigma$  the standard deviation in units of  $10^{-3}$ ,  $\gamma_1$  the skewness, and  $\beta_2$  the kurtosis. A bar above a symbol indicates that it is the average over all the countries in each geographic region, where “Europe” contains countries #1–#23, “America” #24–#31, “Asia” #32–#41, and “Middle East” #42–#48 in Table 1.

Region	Stock Index				Currency			
	$\bar{\mu}$	$\bar{\sigma}$	$\bar{\gamma}_1$	$\bar{\beta}_2$	$\bar{\mu}$	$\bar{\sigma}$	$\bar{\gamma}_1$	$\bar{\beta}_2$
Period 1 (1999–2002)								
Europe	−3.72	6.48	0.03	6.41	−2.48	2.82	−0.09	8.36
America	8.46	6.94	0.43	9.96	−18.25	3.54	−1.89	41.12
Asia	−2.57	6.47	0.57	15.84	−3.47	2.51	−0.03	25.08
Middle East	15.02	5.51	0.17	12.20	−2.87	2.23	−0.18	7.66
Period 2 (2003–2006)								
Europe	38.89	4.48	−0.23	7.4	5.11	2.63	0.07	4.23
America	54.41	4.88	−0.08	6.02	0.02	2.73	−0.42	31.08
Asia	33.22	4.81	−0.52	10.77	−0.42	1.8	−0.02	5.05
Middle East	46.01	5.58	−0.46	44.78	−4.20	2.17	−0.17	4.88
Period 3 (2007–2012)								
Europe	−13.61	7.46	−1.37	50.53	−1.16	3.17	−0.01	7.96
America	14.68	6.91	−0.52	15.13	−3.38	3.49	−4.84	190.62
Asia	10.22	6.06	−0.53	11.34	0.72	2.61	−0.10	10.56
Middle East	6.35	5.79	−0.41	11.17	−2.26	2.65	−0.33	10.59

pairs and for only several possibilities for the trial time-shift values will be quite a daunting task. For example, allowing a six-day delay between a pair will require us to examine  $6N(N-1)/2 \simeq 2.7 \times 10^4$  cases. Granger causality methodology reduces the complexity of calculations by including more than one lag at one time in its regression analysis, but is still characterized as a pairwise analysis. Besides the issue of computational efficiency, furthermore, those methodologies are not appropriate for our targeted network in which nodes are strongly coupled to each other. For instance, one is not able to fully understand the three-body problem by shedding light only on binary relations. To elucidate the multiple relationships in a simultaneous manner, one may think of applying the conventional PCA to time-series each shifted, e.g. with 6 possible time shifts as our pairwise example above. Such an analysis, however, would bring about  $6^N \simeq 5 \times 10^{74}$  cases, an astronomical amount of calculations! In contrast, the CPCA offers tremendous efficiencies, identifying significant lead-lag relationships with just one calculation, as demonstrated in the next section. In addition, the eigenvectors associated with significant eigenvalues, offer insight into different comovement modes in the overall network, not limited to pairwise relationships.

### A. Hilbert transformation and the complexified time series

We first carry out a discrete Fourier expansion of a time series  $r(t)$  ( $t = 1, 2, \dots, T$ ),

$$r(t) = \frac{1}{\sqrt{T}} \sum_{k=1}^T r^{(F)}(k) e^{-i\frac{2\pi}{T}kt}, \quad r^{(F)}(k) = \frac{1}{\sqrt{T}} \sum_{t=1}^T r(t) e^{i\frac{2\pi}{T}kt}, \quad (2)$$

from which it follows that  $r^{(F)}(k) = r^{(F)}(T-k)$ , and that  $r^{(F)}(T) = \sum_{m=1}^T r(t)/\sqrt{T}$  is real.

For even  $T$  the Fourier expansion is written as

$$r(t) = \frac{1}{T} \sum_{t'=1}^T \left(1 + (-1)^{t+t'}\right) r(t') + \frac{2}{\sqrt{T}} \operatorname{Re} \left[ \sum_{k=1}^{T/2-1} r^{(F)}(k) e^{-i\frac{2\pi}{T}kt} \right], \quad (3)$$

where the first term in the left-hand side comes from the  $k = T$  and  $k = T/2$  terms. The Hilbert transform is defined so that it provides the imaginary component of the oscillating part, i.e., the second term on the right-hand side of Eq. (3),

$$r^{(H)}(t) := \frac{2}{\sqrt{T}} \operatorname{Im} \left[ \sum_{k=1}^{T/2-1} r^{(F)}(k) e^{-i\frac{2\pi}{T}kt} \right]. \quad (4)$$

By adding this to the original time series as the imaginary part we obtain a complex time series  $\tilde{r}(t)$ ,

$$\tilde{r}(t) := r(t) + ir^{(H)}(t) = \frac{1}{T} \sum_{t'=1}^T \left(1 + (-1)^{t+t'}\right) r(t') + \frac{2}{\sqrt{T}} \sum_{k=1}^{T/2-1} r^{(F)}(k) e^{-i\frac{2\pi}{T}kt}. \quad (5)$$

Similarly we obtain the following equations for odd  $T$ :

$$r(t) = \frac{1}{T} \sum_{t'=1}^T r(t') + \frac{2}{\sqrt{T}} \operatorname{Re} \left[ \sum_{k=1}^{(T-1)/2} r^{(F)}(k) e^{-i\frac{2\pi}{T}kt} \right], \quad (6)$$

$$\tilde{r}(t) := \frac{1}{T} \sum_{t'=1}^T r(t') + \frac{2}{\sqrt{T}} \sum_{k=1}^{(T-1)/2} r^{(F)}(k) e^{-i\frac{2\pi}{T}kt}. \quad (7)$$

Note that both Eqs. (5) and (7) rotate clockwise in the complex plane.

### B. Complex Correlation Matrix

The normalized log-return  $\tilde{w}_\alpha$  for the complex time series  $\tilde{r}_\alpha(t)$  is defined by

$$\tilde{w}_\alpha(t) := \frac{\tilde{r}_\alpha(t) - \langle \tilde{r}_\alpha \rangle_t}{\sigma_\alpha}, \quad (8)$$

where  $\langle \cdot \rangle_t$  is the average over time  $t = 1, \dots, T$  ( $\langle \cdot \rangle_t := (1/T) \sum_{t=1}^T \cdot$ ), and  $\sigma_\alpha (\geq 0)$  is the standard deviation of  $\tilde{r}_\alpha$  over time,

$$\sigma_\alpha^2 := \frac{1}{T} \sum_{t=1}^T |\tilde{r}_\alpha(t) - \langle \tilde{r}_\alpha \rangle_t|^2 = \langle |\tilde{r}_\alpha|^2 \rangle_t - |\langle \tilde{r}_\alpha \rangle_t|^2. \quad (9)$$

The complex correlation matrix  $\tilde{\mathbf{C}}$  is an  $N \times N$  ( $N = 96$ ) Hermitian matrix defined as

$$\tilde{\mathbf{C}}_{\alpha\beta} := \langle \tilde{w}_\alpha \tilde{w}_\beta^* \rangle_t, \quad (10)$$

whose diagonal elements are 1 by definition of the normalized log-return  $\tilde{w}_\alpha$  (Eq. (8)).

The eigenvalues  $\lambda^{(n)}$ , which are non-negative due to the chirality of the Hermitian matrix  $\tilde{\mathbf{C}}$ , and the corresponding eigenvectors  $\mathbf{V}^{(n)}$  of the matrix  $\tilde{\mathbf{C}}$  satisfy the following relations,

$$\tilde{\mathbf{C}} \mathbf{V}^{(n)} = \lambda^{(n)} \mathbf{V}^{(n)}, \quad (11)$$

$$\mathbf{V}^{(n)*} \cdot \mathbf{V}^{(m)} = \delta_{nm}, \quad (12)$$

$$\sum_{n=1}^N \lambda^{(n)} = N, \quad (13)$$

$$\tilde{\mathbf{C}} = \sum_{n=1}^N \lambda^{(n)} \mathbf{V}^{(n)} \mathbf{V}^{(n)\dagger}. \quad (14)$$

The superscripts in parentheses such as  $(n)$  denote the indices of different eigenvalues and eigenvectors, having the range  $n = 1, \dots, N$ . We order the eigenvalues in descending order  $\lambda^{(n)} \geq \lambda^{(n-1)}$ , for any  $n$ . Here  $\delta_{nm}$  is the Kronecker delta, i.e.,  $\delta_{nm} = 1$  if  $n = m$ ,  $\delta_{nm} = 0$  if  $n \neq m$ . Eigenmodes with large eigenvalues are the key to uncovering co-movements in this set of time series. This is the case because when the time series are expanded in terms of the eigenvectors,

$$\tilde{w}_\alpha(t) = \sum_{n=1}^N a^{(n)}(t) \mathbf{V}_\alpha^{(n)}, \quad (15)$$

the mode-signals  $a^{(n)}(t)$  satisfy

$$\langle a^{(n)*} a^{(m)} \rangle_t = \delta_{nm} \lambda^{(n)}, \quad (16)$$

which can be proven using Eqs. (10), (11), and (12). Equation (16) shows that the larger the eigenvalue the larger will be the presence of the eigenvector, with their mean strength proportional to the square root of the eigenvalues. The next question is how to determine which eigenmodes (with large eigenvalues) are significant, i.e., which are free from noise.

Because in our case  $T$  is odd, we expand the normalized log-return  $\tilde{w}_\alpha$  as

$$\tilde{w}_\alpha(t) = \frac{2}{\sqrt{T}} \sum_{k=1}^{(T-1)/2} w_\alpha^{(F)}(k) e^{-i\frac{2\pi}{T}kt}, \quad (17)$$

in a way similar to that in Eq. (7). Substituting this into Eq. (10), we find that

$$\tilde{C}_{\alpha\beta} := \frac{4}{T} \sum_{k=1}^{(T-1)/2} w_{\alpha}^{(F)}(k) w_{\beta}^{(F)}(k)^* = \frac{4}{T} \sum_{k=1}^{(T-1)/2} \left| w_{\alpha}^{(F)}(k) w_{\beta}^{(F)}(k)^* \right| e^{i(\delta_{\alpha}(k) - \delta_{\beta}(k))}, \quad (18)$$

where  $\delta_{\alpha}(k)$  is the phase of  $w_{\alpha}^{(F)}(k)$ . Thus when there is only one Fourier-component in either  $\tilde{w}_{\alpha}(t)$  or  $\tilde{w}_{\beta}(t)$ , the phase of the complex correlation coefficient  $\tilde{C}_{\alpha\beta}$  is equal to  $T/(2\pi k)$  times the amount of *delay* of the time series  $\tilde{w}_{\alpha}(t)$  relative to  $\tilde{w}_{\beta}(t)$  (in that Fourier mode). If there are multiple Fourier components, the phase of the complex correlation coefficient  $\tilde{C}_{\alpha\beta}$  is a weighted (non-linear) average of the time-delay as in Eq. (18). When  $T$  is even, a similar relation holds.

### C. Rotational Random Shuffling (RRS) method

As explained in detail in Iyetomi et al. (2011), several methods can be used to establish which eigenmodes are important when extracting significant information from related time series. Random matrix theory (RMT) results for the spectrum of iid (independent, identically distributed) time series (Marčenko and Pastur (1967)) clearly indicate that a time series that is truly random induces a nontrivial spectrum of eigenvalues. The RMT method is not suitable for our purpose, however, (i) because there are many autocorrelations in each of the time series analyzed and (ii) because 12 European countries (#2 through #11 in Table 1) adopted the Euro in January 1999 and their currency time series is thus identical by definition. Because the drachma was closely related to the Euro before Greece (#12 in Table 1) adopted the Euro in 2001, its currency time series are very close to those of the other European countries. Because of these characteristics in our data, there are eleven zero eigenvalues and one eigenvalue close to zero, and there are a number of artificially large eigenvalues due to the constraint in Eq. (13).

We thus use the RRS simulation proposed in Arai and Iyetomi (2013), not RMT, to extract a meaningful spectrum of significant eigenvalues. In this simulation we first randomly rotate each time series (with the currencies of 11 European countries from Austria to Greece in Table 1) as

$$\tilde{w}_{\alpha}(t) \rightarrow \tilde{w}_{\alpha}(\text{Mod}(t - \tau_{\alpha}, T) + 1), \quad (19)$$

where

$$\tau_{\alpha} = \begin{cases} 0, & \text{for } \alpha = 50, \dots, 60, \\ (\text{pseudo-})\text{random integer} \in [0, N], & \text{otherwise.} \end{cases} \quad (20)$$

We then obtain eigenvalues  $\lambda^{(n)}$  from the rotated time series. In this way we keep the autocorrelation of individual time series intact but cancel out co-movements between the time series (except the trivial co-movements among the 11 European countries that use the common Euro currency). Thus by comparing the resulting shuffled eigenvalue spectrum with the original eigenvalue set we can identify the important, non-random co-movements within the equity-currency coupled network.

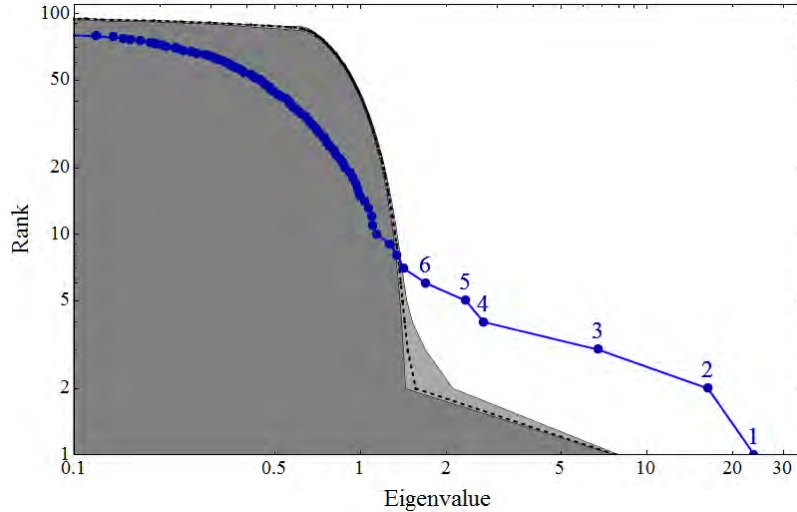


**Figure 1. Significant eigenvalues identified by the CPCA with RRS results.** The blue dot denoted “ $n$ ” shows the  $n$ -th largest CPCA eigenvalue ( $x$ -axis) and the CPCA eigenvalue rank ( $y$ -axis). The gray small dots and the lighter gray area show the average RRS and the 99% range. The six largest eigenvalues are clearly outside of their RRS ranges, and show significant relationships in the interdependent network.

### III. Interdependent Network Analysis

The eigenvalues obtained using CPCA (the large dots with numbers and the blue line) and the RRS results (the small dots and the dashed line) are plotted in Fig. 1 and displayed in Table 4. The first six eigenvalues, #1–#6, lie outside the RRS 99% error-range and thus are clearly identifiable. These six largest eigenvalues can be used to explain the significant co-movements in the system. For periods 1–3, similar analyses show that 5 CPCA eigenvectors are significant (see Appendix A, Fig. A1).

As discussed above, because CPCA is able to detect cross-correlations with lead-lag relations in multivariate time series it should, in theory, be superior to a conventional PCA-based analysis. Figure 2 shows that, in practice, CPCA is in fact superior to PCA and that the cumulative sum of the CPCA eigenvalues is consistently larger than that of the PCA eigenvalues.

#### A. Properties of the dominant eigenmodes

Using CPCA analysis we identify the dynamics of the eigenvector components of the six largest eigenvalues, we plot the first three in Figs. 3-5, and observe the following;

Figure 3 shows the causal relationship between the stock markets and the currencies in the 48 countries we analyze in this study during the entire 1999–2012 period. The behavior of the eigenvector components corresponding to the largest eigenvalues indicates that currency performance usually leads or influences stock market

**Table 4: List of CPCA Eigenvalues, their 99% RRS Range, and the mean contribution rate  $\sqrt{\lambda^{(n)}/\lambda^{(1)}}$  as in Eq. (16).** Although the seventh eigenmode is outside the RRS range, we exclude this mode as insignificant as it is very close to the boundary.

$n$	$\lambda^{(n)}$	99% RRS range	$\sqrt{\lambda^{(n)}/\lambda^{(1)}}$
1	23.74	$7.79^{+0.17}_{-0.02}$	1
2	16.35	$1.56^{+0.54}_{-0.12}$	0.83
3	6.76	$1.46^{+0.22}_{-0.05}$	0.53
4	2.69	$1.42^{+0.09}_{-0.03}$	0.37
5	2.33	$1.40^{+0.05}_{-0.03}$	0.31
6	1.69	$1.38^{+0.03}_{-0.02}$	0.27
7	1.41	$1.36^{+0.03}_{-0.02}$	0.24
8	1.35	$1.35^{+0.02}_{-0.02}$	0.24

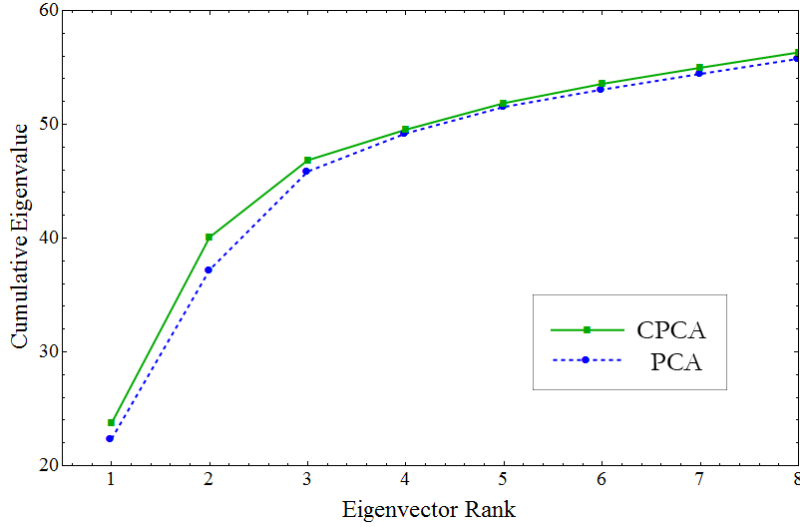


**Figure 2. Comparison between the PCA and CPCA eigenvalues.** In each case, the partial sum of the eigenvalues,  $\sum_{n=1}^K \lambda^{(n)}$  ( $y$ -axis) versus  $K$  ( $x$ -axis), for PCA (blue and dashed) and for CPCA (green and solid). The fact that the CPCA sums of eigenvalues are always above PCA-based eigenvalue sums shows that CPCA is a stronger analytic tool in identifying important co-movements.

performance in each of the countries.

The US financial market is clearly a leader or indicator of the future performance of other global financial markets. The US equity markets, closely followed by German and UK equity markets, are predictive of the performance of equity markets in the other countries of our study. During the 1999–2002 mild crisis period the US, Germany, and UK equity markets are also leaders in forecasting currency returns.

During the calm 2003–2006 period financial markets do not exhibit strong correlations but currency markets do. Asian and South American currencies as well as the US dollar are predictive of the performance of the Euro, British Pound, Canadian Dollar, and Japanese Yen.

The severe 2007–2012 crisis period strongly resembles the entire 1999–2012 period, indicating that this period strongly influences market trends and currency market-equity market interdependencies throughout the period. Findings based on largest-eigenvalue analysis agree with the importing firm (or country) theory, i.e., that an appreciation in a local currency lowers the price of imported goods to the firm or country and increases profits realized in future payables to the firm or country—the payables being denominated in foreign currency—and thus increases the equity value of the importing firm or country. This in turn has a positive impact on equity markets.

Figure 4 shows the behavior of the eigenvector components corresponding to the second largest eigenvalue. Equity markets and currency markets exhibit an equal-time (concurrent) negative correlation, and this is particularly strong in the US, German, UK, and Canadian markets. There are also strong geographical positive correlations in which separate clusters are formed by the European and Asian equity markets. Note also that Asian equity markets are predictive of their corresponding currency markets.

During the 1999–2002 mild crisis period currency markets are predictive of equity market performance. During the calm 2003–2006 period this predictive power of currency markets is somewhat diminished. The severe 2007–2012 crisis period exhibits behavior similar to the entire analyzed period, once again dominating the equity-currency causal relationship that we observe for the entire 1999–2012 period.

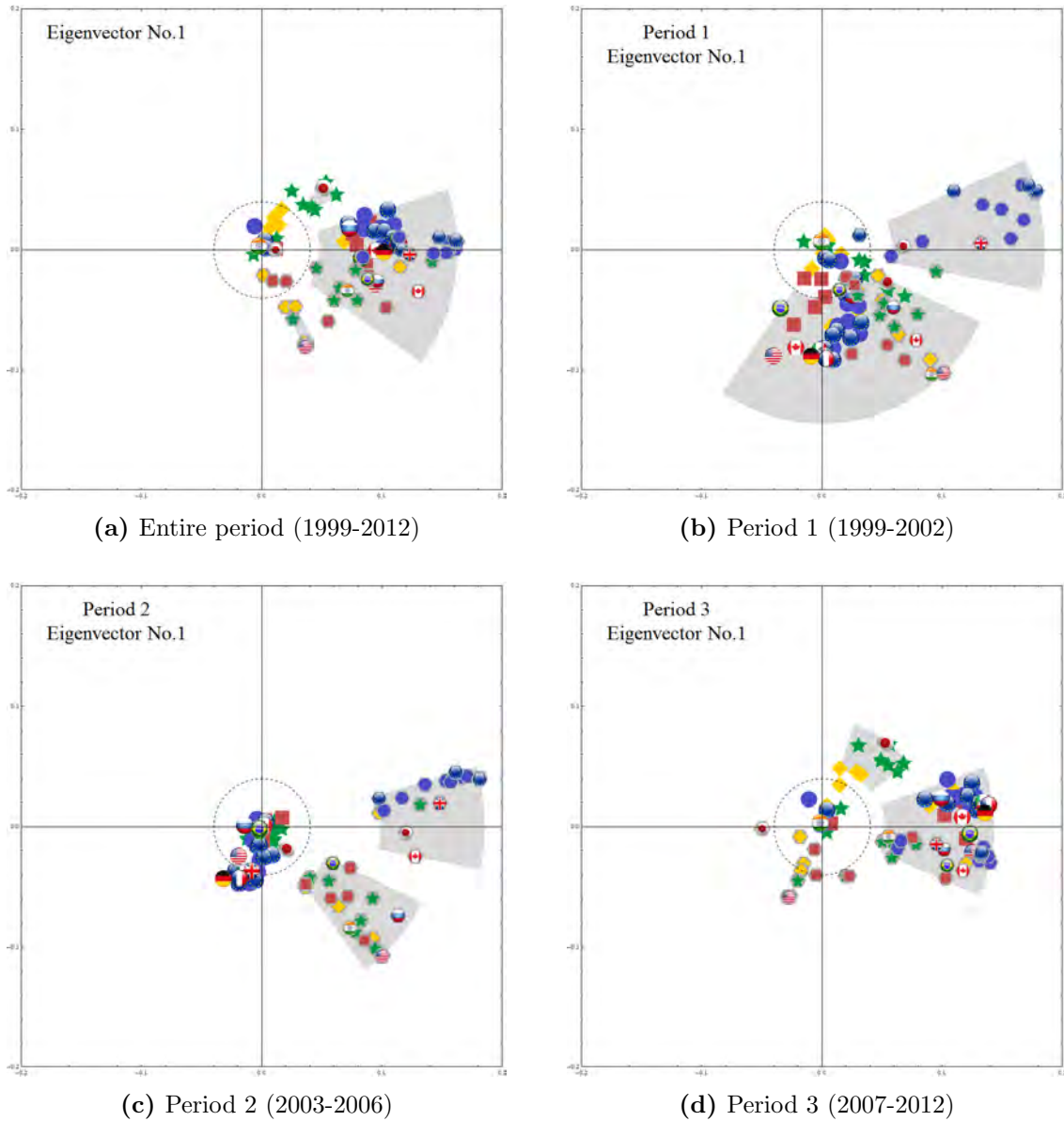
We see that positive performances in the US, UK, German, and Canadian financial markets are frequently linked to a simultaneous depreciation of the nation’s currency. Although we would expect a local currency to be in higher demand when an equity market increases and thus to appreciate, increases in the equity market can also be driven by domestic (not international) investors. Other factors can also affect equity and currency markets, including quantitative easing, inflation, and fluctuating interest rates. Coupling a weaker currency with a strong equity market is a tactic advocated by the trade-dominant theory in which a government protects its currency by artificially depreciating it in order to boost exports and maintain stability in the foreign exchange market.

The results for Asia and South America indicate that when the performance of a country’s financial markets is positive, the country’s currency appreciates (with a time lag) because the desirable investment climate has increased demand for the

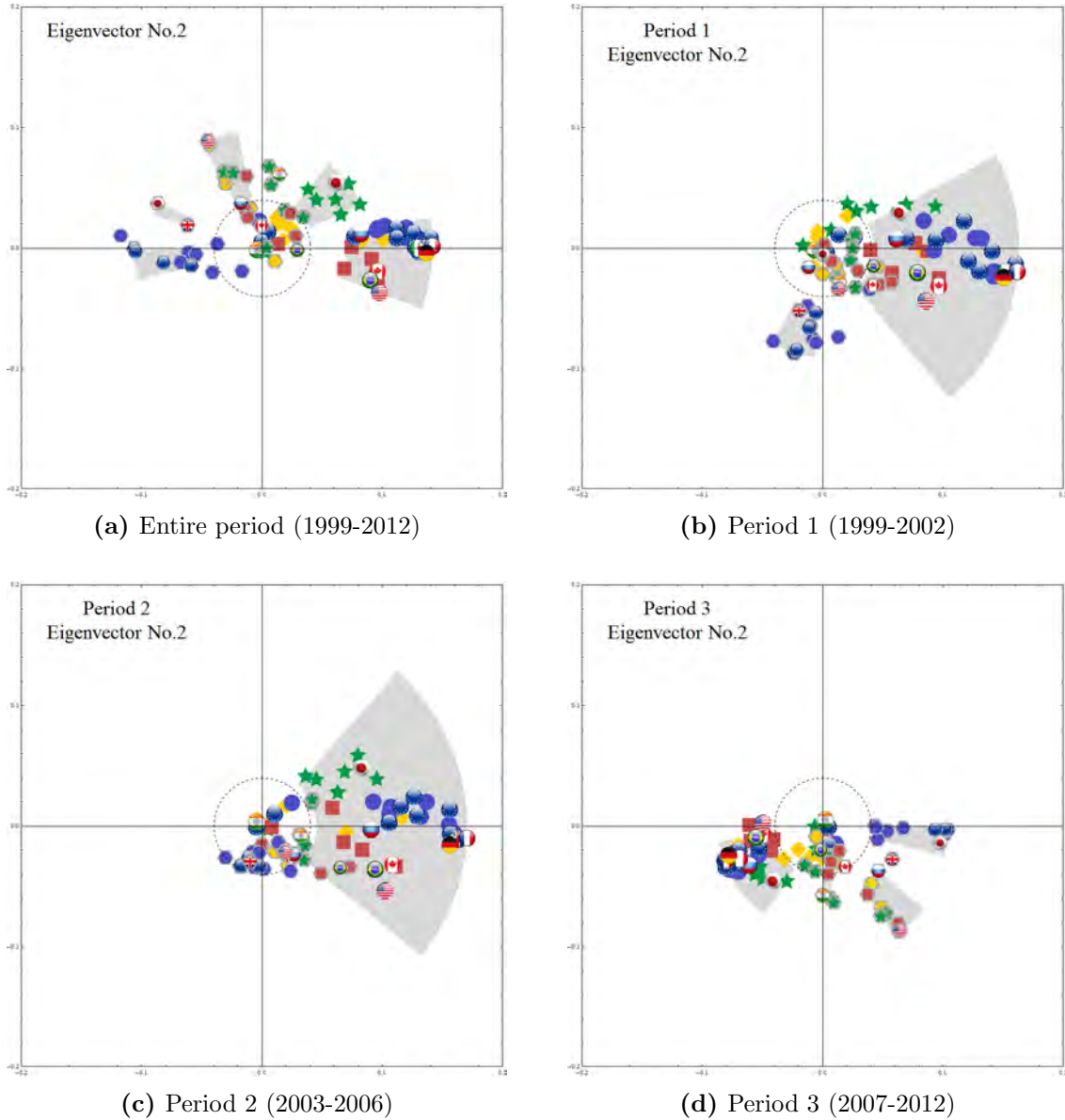
currency by investors following a balanced portfolio strategy Pan et al. (2007).

Figure 5 shows the third eigenvector components. There are two large clusters, one containing most of the European currencies and the other the Asian, South American, and Middle Eastern currencies, largely dominated by the US dollar. Note that here the correlation among stock market indices is almost non-existent, and that the causal relationships for the entire period and the three subperiods are similar.





**Figure 3. The 1st eigenvector (whose eigenvalue is the largest) components on a complex plane.** The flags without the gray background represent the equity markets, while the dark gray hexagons behind the flags represent the currencies as shown in Table 1. The nodes with absolute value larger than 0.04 (which is indicated with a dashed circle) are grouped so that nodes with phase gap greater than 0.2 [rad] are classified to separate groups. Plot (a) for the entire period shows that currencies lead by the US dollar precede the global stock markets, among which the US, German and Canadian markets are leaders of other countries' equity markets. While these features are also seen in the severe crisis period (Period 3), during other calmer periods, we observe lower correlation between stock markets.



**Figure 4. The components of the 2nd eigenvector** (corresponding to the second largest eigenvalue  $\lambda^{(2)}$ ), multiplied (scaled) by the ratio of the corresponding mode-signals,  $\sqrt{\lambda^{(2)}/\lambda^{(1)}}$  reflecting the fact that the strength of the contribution of the  $n$ -th eigenmode to the time series is proportional to the  $\sqrt{\lambda^{(n)}}$  (see Eq. (16)). For the entire period, the currency markets are distributed to the left of the origin, mainly close the negative real axis, while equity markets are along the positive real axis and also in the first quadrant, indicating negative equal-time correlation between the equity and foreign exchange markets. Again, these features are almost the same for Period 3, the severe crisis period, and differs in other periods.

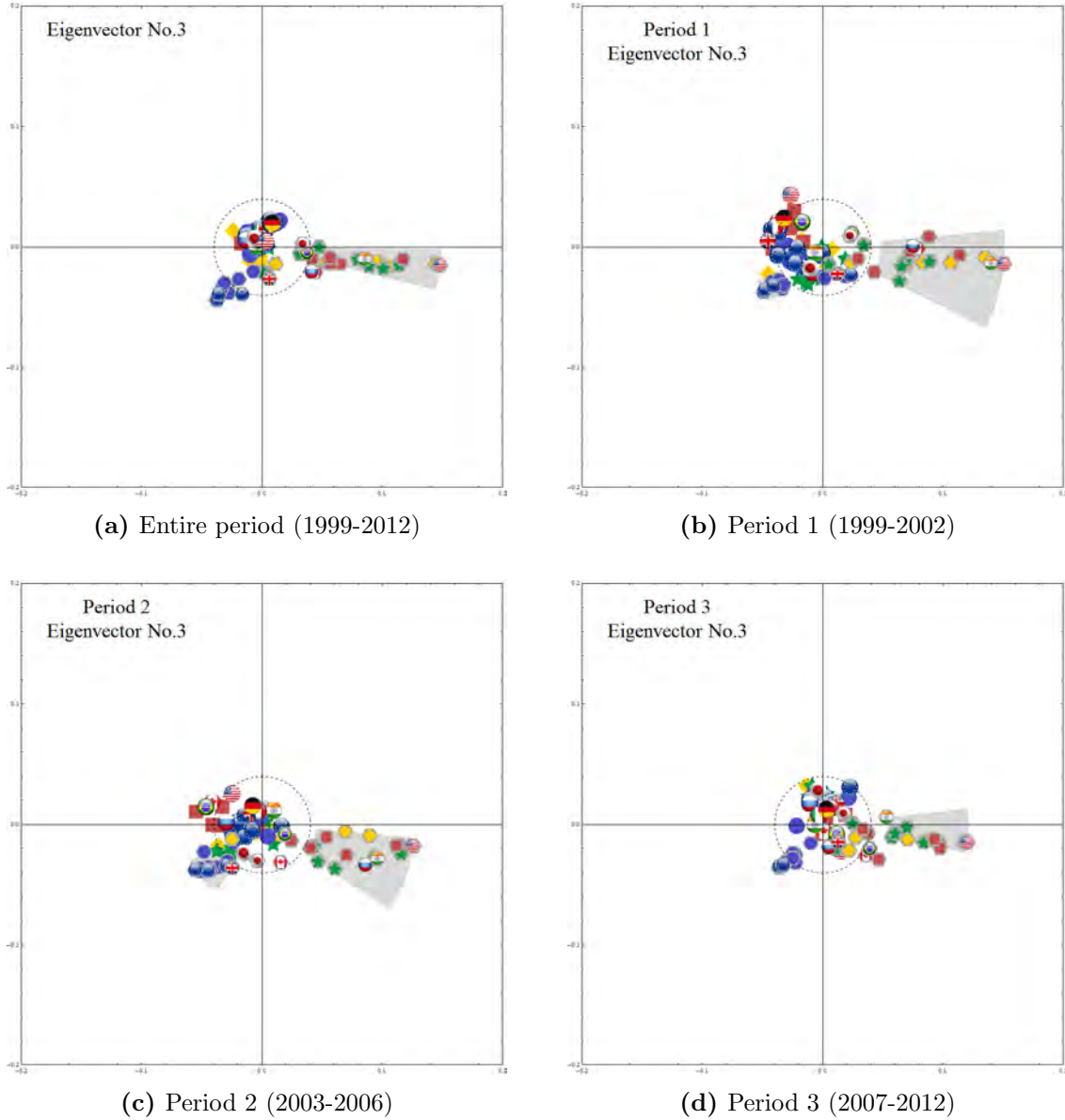


**Figure 5. The 3rd eigenvector components, multiplied by  $\sqrt{\lambda^{(3)}/\lambda^{(1)}}$ .** We observe two clusters, one of consisting of European currencies, and the other being dominated by the US dollar and Asian, South American and Middle Eastern currencies. The two clusters have negative equal-time correlation. Curiously, this behavior is universal, *i.e.*, is common for all the periods.

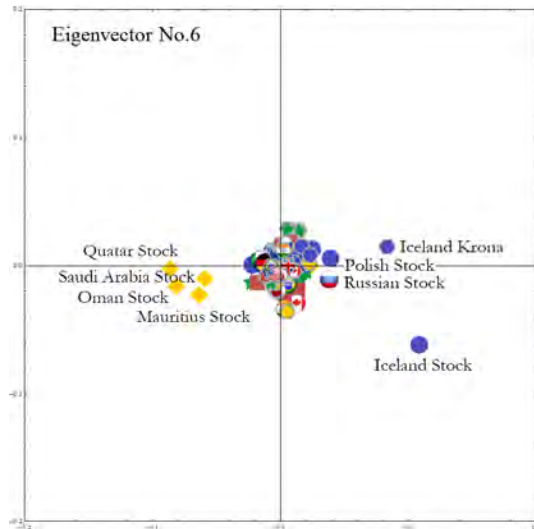


**Figure 6.** The 6th eigenvector components, multiplied by  $\sqrt{\lambda^{(6)}/\lambda^{(1)}}$ , with names for the nodes that have large absolute values for the entire period. We observe that this eigenmode has the largest contribution of Iceland’s stock market, followed by the Icelandic Krona. Closely following Iceland, are Polish and Russian stock markets with positive correlation and oil-stocks with negative correlation.

### B. Insights from smaller significant eigenmodes

In the previous section we examined the dominant relationships between stock markets and currencies within the first, second, and third eigenvectors. In our network analysis, however, we have identified a total of six significant eigenvalues. The last column of Table 4 shows that the smaller eigenvalues (4–6) contribute much less (approximately 30% of the first eigenmode) to explaining currency-equity network dynamics. Thus *on average* the fourth, fifth, and six eigenmodes are much less important than the first three.

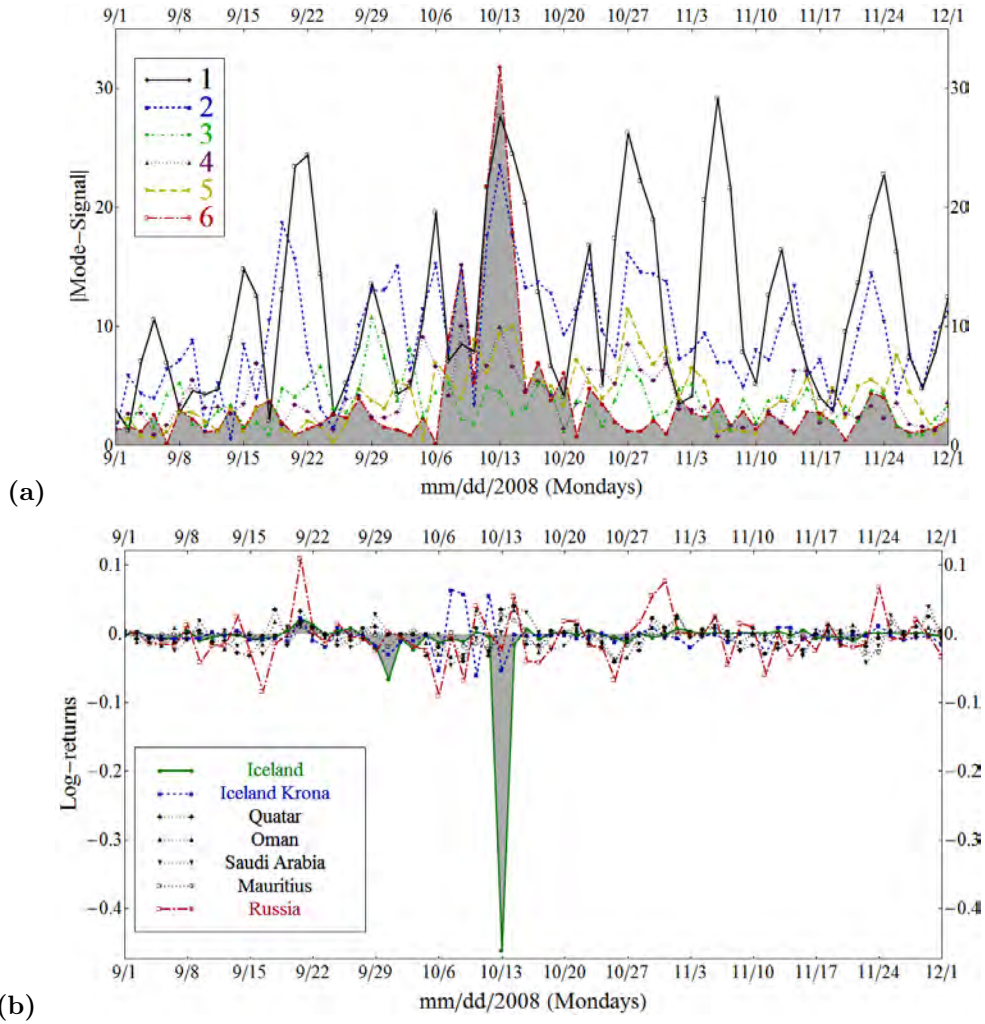
Note the proximity of the fourth and fifth eigenvalues, which means that these eigenmodes are approximately *degenerate* and that any linear combination of these two eigenvectors are close to being one eigenvector. Thus a separate examination of the fourth and fifth eigenvectors may produce no useful results.

Figure 6 shows the sixth eigenvector components that dominate the dynamics of the stock and foreign exchange market behavior, including the Icelandic Krona and the Icelandic, Polish, and Russian stock markets on one side and the Middle Eastern stock markets on the other.

Figure 6 also shows that on October 13, 2008, the day when the Icelandic financial crisis hit, this sixth eigenmode has a stronger influence than even the first eigenmode. Figure 7(b) shows that the log-return of the Icelandic stock market (the green line with the shaded gray area) dips sharply. On this day the Icelandic stock market lost over 90% of its market capitalization and contributed to the collapse of all three of Iceland’s major financial institutions, creating unprecedented social unrest and

initiating a major economic and political crisis. According to *The Economist* of December 11, 2008, relative to the size of its economy Iceland's collapse was the largest in economic history (The Economist (2008)).

This demonstrates the strength of our CPCA and RRS based analysis and its sensitivity to such world events as the Icelandic financial crisis. Although it was localized in time and occurred in only a couple of time series out of 96, our analysis did not exclude this occurrence as noise and was able to identify this Icelandic stock market event as a signal of importance in the sixth eigenmode.



**Figure 7. Log-returns and mode-signals of the 6th eigenvector selected components** (a) Absolute values of the mode-signals for the eigenmodes 1 to 6 from September 1st to December 1st of 2008 (The ticks for the x-axis are given only for Mondays). The red dots connected with red dash-dot lines show that the 6th eigenmode, which is evidently significant on October 13th, exceeds the contribution of the 1st eigenmode. As we saw in Fig. 6, the 6th eigenmode is singular in the sense that while its average contribution to the whole set of the time series is small (as  $\sqrt{\lambda^{(6)}/\lambda^{(1)}} \simeq 0.24$  in Table 4), it has a limited number of nodes with large absolute values lead by Iceland's stock market and the Icelandic Krona. In this plot we observe that this 6th eigenmode has large contribution in the time-signal at the time of Iceland's financial crisis, even exceeding that of the first eigenmode. (b) Behavior of the log-returns of the time series that have large absolute values in the 6th eigenvector. This plots shows that in fact the actual time series of the dominant nodes in the 6th eigenmode has significant signal at the Iceland's banking crisis, which is consistent with the large mode-signal observed above.

#### IV. Community Analysis

An alternative way of studying the time-averaged aspects in the collective behaviors of the financial constituents is to construct a network based on our CPCA analysis and explore the formation of distinct network communities. For this purpose, we study the filtered complex correlation coefficients,

$$\tilde{C}_{\alpha\beta}^{(N_s)} = \sum_{n=1}^{N_s} \lambda^{(n)} \mathbf{V}_\alpha^{(n)} \mathbf{V}_\beta^{(n)\dagger} = r_{\alpha\beta} e^{i\theta_{\alpha\beta}}, \quad (21)$$

where  $\tilde{C}_{\alpha\beta}^{(N_s)}$  is a correlation coefficient obtained by retaining only the  $N_s$  ( $N_s = 6$  for the entire period and period three and  $N_s = 5$  for periods one and two dominant eigenvalues and their associated eigenvectors in the spectral decomposition of Eq. (14), while  $r_{\alpha\beta}$  and  $\theta_{\alpha\beta}$  are the magnitude and phase of the correlation coefficient, respectively.

We consider the correlation matrix  $\tilde{C}^{(N_s)}$  as an adjacency matrix, and construct a network of the financial nodes linked to each other with the corresponding correlation coefficients as (complex) weights.

The network thus constructed is in principle a complete graph in which all pairs of nodes are connected. However the coupling strength between nodes  $\alpha$  and  $\beta$  varies with their associated magnitude  $r_{\alpha\beta}$  ranging from 0 to 1. Note that the linkage has direction depending on the lead-lag relation between the two nodes:  $\beta$  ( $\alpha$ ) leads  $\alpha$  ( $\beta$ ) if  $\theta_{\alpha\beta}$  takes a positive (negative) value. Here we define the directed links of each pair to be between the leader and the follower. The in-degree  $k_\alpha^{\text{in}}$  and the out-degree  $k_\alpha^{\text{out}}$  of node  $\alpha$  are hence calculated as

$$k_\alpha^{\text{out}} = \sum_{\beta(\theta_{\alpha\beta} < 0)} r_{\alpha\beta}. \quad (22)$$

$$k_\alpha^{\text{in}} = \sum_{\beta(\theta_{\alpha\beta} > 0)} r_{\alpha\beta}, \quad (23)$$





















By calculating

$$\Delta k_\alpha = k_\alpha^{\text{out}} - k_\alpha^{\text{in}}, \quad (24)$$

we can single out four typical cases for nodes with different lead-lag relations, (i)  $k_\alpha^{\text{out}} \gg k_\alpha^{\text{in}}$ , (ii)  $k_\alpha^{\text{out}} \ll k_\alpha^{\text{in}}$  (see the first and second half of Table 5 respectively), (iii)  $k_\alpha^{\text{out}} \simeq k_\alpha^{\text{in}} \neq 0$ , and (iv)  $k_\alpha^{\text{out}} \simeq k_\alpha^{\text{in}} \simeq 0$  (see Table 6). The stock markets and currencies satisfying condition (i) lead the world economy. Those satisfying condition (ii) follow the leaders. Those satisfying condition (iii) are sometimes leaders and sometimes followers. Those satisfying condition (iv) are nodes that are for the most part isolated from the rest of the world.

Table 5 shows that the US and the German stock markets and the Mexican Peso and the Australian Dollar are the strongest leaders in the stock market-foreign exchange coupled network during the 1999–2012 period. Note that the Mexican Peso

**Table 5: Top 10 and bottom 10 nodes by  $k^{\text{out}} - k^{\text{in}}$  for the entire period (1999-2012).** Note that node indices larger than 48 are for currencies; for example, node index 74 is the currency for Mexico, or country #26 (= 74 - 48) in Table 1.

Node Index	Marker	Node Name	$k^{\text{out}}$	$k^{\text{in}}$	$k^{\text{out}} - k^{\text{in}}$
24		USA	22.6	2.0	20.6
74		Mexican Peso	22.7	3.2	19.5
6		Germany	20.6	4.8	15.8
89		Australian Dollar	22.3	7.1	15.2
73		Canadian Dollar	21.8	6.8	15.0
75		Brazilian Real	17.4	3.3	14.1
92		Saudi Riyal	18.5	4.5	14.0
93		South African Rand	19.2	5.3	13.8
1		UK	20.7	6.9	13.8
26		Mexico	18.2	4.5	13.6
37		Malaysia	1.4	12.7	-11.4
41		Australia	4.4	16.5	-12.2
61		Maltese Lira-Euro	4.6	17.2	-12.6
35		Japan	3.0	15.9	-12.8
39		Philippines	1.2	14.1	-12.8
19		Czech	5.0	18.1	-13.2
63		Norwegian Krone	6.9	22.4	-15.5
60		Greek Drachma-Euro	6.3	22.6	-16.3
62		Slovak Koruna-Euro	4.8	22.3	-17.5
2		Austria	4.5	22.5	-17.9





















co-moves closer to the US market than the US dollar because during this entire period the Mexican Peso and the US stock market are peripheral to their communities, while the US dollar is a core node of the community to which the Mexican Peso belongs. In period 3, the Mexican Peso and the US market are identified as members of the same community. During this period the Euro and some of the other European currencies are the ones most influenced by the rest of the global stock markets and currencies.

Table 6 shows that the extent to which the Italian, Dutch, and Finish stock markets are influenced by other markets and currencies are similar to the extent to which they influence other stock markets and currencies. The Slovakian, Indian, and South Korean markets are the most isolated from the rest of the world, and neither significantly affect other markets nor are influenced by them. For a more elaborate listing of leaders and followers in the coupled forex-stock market network for the entire period (1999–2012) and the three subperiods (1999–2002), (2003–2006), and (2007–2012), see Vodenska et al. (2014).

During the 1999–2002 and 2003–2006 periods the US and German stock markets exhibit the largest  $\Delta k$  values and lead the world economy. During the 2007–2012 period, however, they are replaced by the currencies of such developing countries as Mexico, South Africa, and Brazil. On the other hand, during the 1999–2002 and 2003–2006 periods the European currencies are followers that exhibit large negative  $\Delta k$  values, the most affected during 1999–2002 being the Greek Drachma (prior to



**Table 6: Stock markets and currencies with the lowest absolute differences  $|k^{\text{out}} - k^{\text{in}}|$  for the entire period (1999-2012).** We have ordered the components in descending order of  $(k^{\text{out}} + k^{\text{in}})$  to show the relative position of stock markets and currencies in the coupled network.

Node Index	Marker	Country	$k^{\text{out}}$	$k^{\text{in}}$	$k^{\text{out}} - k^{\text{in}}$	$k^{\text{out}} + k^{\text{in}}$
8		Italy	13.6	13.7	-0.1	27.3
9		Netherlands	14.5	12.5	2.1	27.0
4		Finland	13.0	13.5	-0.5	26.5
66		Swiss Franc	12.2	11.2	1.0	23.4
85		Malaysian Ringgit	12.9	10.4	2.5	23.3
77		Chilean Peso	12.0	9.3	2.7	21.3
80		Indian Rupee	10.3	11.1	-0.8	21.3
28		Argentina	9.6	9.7	-0.1	19.4
87		Philippines Peso	10.3	8.9	1.5	19.2
86		Thai Baht	9.2	8.9	0.3	18.1
42		Israel	9.9	7.7	2.2	17.7
82		Indonesian Rupiah	5.6	7.9	-2.3	13.5
47		Qatar	2.5	5.5	-3.0	7.9
33		Sri Lanka	0.6	4.2	-3.6	4.8
43		Pakistan	0.5	3.4	-2.9	4.0
31		Venezuela	2.2	1.4	0.7	3.6
13		Malta	0.4	2.7	-2.4	3.1
36		South Korea	2.3	0.2	2.1	2.6
32		India	0.8	1.4	-0.6	2.2
14		Slovakia	0.7	0.9	-0.2	1.6

the adoption of the Euro in 2001), the Hungarian Forint, and the Czech Republic Koruna, and the most affected during 2003–2006 the Slovak Koruna (prior to the adoption of the Euro in 2009), the Norwegian krone, and the Swedish Krona. During the 2007–2012 period stock markets generally follow currency markets, with the stock markets of Austria, Philippines, and Hungary exhibiting the largest negative  $\Delta k$  values.

To further understand this synchronization in economic relations, we impose the following condition on each pair of nodes  $\alpha$  and  $\beta$  we want to connect:

$$|\theta_{\alpha\beta}| < \theta_c . \quad (25)$$

By proposing that the weight of the link between the nodes be given by the magnitude  $r_{\alpha\beta}$  we are able to construct a synchronization network in which nodes moving in phase are linked to each other.

#### A. Community structure

Community detection, the extraction of nodes tightly connected as communities, is widely used to identify clustering structures in complex networks. Here a community is a collection of co-moving nodes. Setting  $\theta_c/\pi = 0.1$  in Eq. (25), we obtain the synchronization networks in the entire period and in the three subperiods. Maximizing the modularity and identifying the network communities, we find that the network has a meaningful community structure in each period with modularity values of 0.415 (1999–2012), 0.516 (1999–2002), 0.556 (2003–2006), and 0.348 (2007–2012). In practice, modularity values exceeding approximately 0.3 indicate that community decomposition is significant (Newman and Girvan (2004)). Details of the community detection algorithm are described in Appendix C, including the sensitivity of the community structure to different cutoff values for  $\theta_c$ .

We can clearly see the community structure in Table 7 and Fig. 8. In the following sections we will denote the community  $\#n$  in Table 7 as  $Cn$ .

Note that the community structure of the stock market and foreign exchange coupled network is relatively stable over both the entire period and the three subperiods, i.e., the 1999–2002 (mild crisis), 2003–2006 (calm period), and 2007–2012 (severe crisis) periods. We thus classify the financial constituents into four dominant communities:

1. The stock market community C1, dominated by Europe, South America, the USA, and Canada as major categories that always appear in this community;
2. The currencies-only community C2, dominated by Europe and Canada;
3. The currency community C3, dominated by Russia, the USA, South America, Asia, and the Middle East; and
4. The stock market community C4, dominated by Asia (including Japan) and the Middle East.

**Table 7: Results of the community detection for the entire period (1999-2012) and in the three characteristic periods (period 1: 1999-2002, period 2: 2003-2006, and period 3: 2007-2012).** The stock markets and currencies of 48 countries are decomposed into four co-moving communities, designated by numbers (“IN” means an independent node), in each period.

No.	Country	Whole Period		Period 1		Period 2		Period 3	
		Stock	Currency	Stock	Currency	Stock	Currency	Stock	Currency
1	UK	1	2	1	2	1	2	1	2
2	Austria	1	2	1	2	1	2	1	2
3	Belgium	1	2	1	2	1	2	1	2
4	Finland	1	2	1	2	1	2	1	2
5	France	1	2	1	2	1	2	1	2
6	Germany	1	2	1	2	1	2	1	2
7	Ireland	1	2	1	2	1	2	1	2
8	Italy	1	2	1	2	1	2	1	2
9	Netherlands	1	2	1	2	1	2	1	2
10	Portugal	1	2	1	2	1	2	1	2
11	Spain	1	2	1	2	1	2	1	2
12	Greece	1	2	4	2	1	2	1	2
13	Malta	3	2	1	2	3	2	2	2
14	Slovakia	1	2	1	2	4	2	3	2
15	Norway	1	2	1	2	1	2	1	2
16	Sweden	1	2	1	2	1	2	1	2
17	Iceland	3	2	4	2	4	2	IN	2
18	Switzerland	1	2	1	2	1	2	1	2
19	Czech	1	2	1	2	1	2	1	2
20	Denmark	1	2	1	2	1	2	1	2
21	Hungary	1	2	1	2	1	2	1	2
22	Poland	1	2	4	2	1	2	1	2
23	Russia	1	3	4	3	1	3	1	2
24	USA	1	3	1	3	1	3	2	3
25	Canada	1	2	1	3	1	2	1	2
26	Mexico	1	3	1	3	1	3	1	2
27	Brazil	1	2	1	1	1	3	1	2
28	Argentina	1	3	1	3	1	3	1	3
29	Chile	1	3	1	3	1	3	1	1
30	Peru	1	3	1	3	4	3	1	3
31	Venezuela	1	3	1	3	1	3	2	3
32	India	3	3	1	3	3	3	2	3
33	Sri Lanka	4	3	4	3	3	3	4	3
34	Indonesia	4	3	4	3	4	3	4	3
35	Japan	4	2	4	2	4	2	4	2
36	Korea	3	3	IN	3	1	3	2	1
37	Malaysia	4	3	4	3	4	3	4	3
38	Thailand	4	3	4	3	4	3	4	3
39	Philippine	4	3	4	3	4	3	4	3
40	Hong Kong	4	3	4	3	4	3	4	3
41	Australia	4	2	4	2	4	2	4	2
42	Israel	1	3	1	3	1	3	1	3
43	Pakistan	4	3	4	3	4	3	4	3
44	Saudi Arabia	4	3	4	3	1	3	3	3
45	South Africa	1	2	1	3	1	2	1	2
46	Oman	4	3	3	3	4	3	4	3
47	Qatar	4	3	2	3	3	3	4	3
48	Mauritius	4	3	1	3	4	3	4	3



**Figure 8. Geographical distribution of the community structure for the entire period given in Table 7** including the communities dominated by stock markets with red and orange colors and communities dominated by mainly currencies with blue and green colors

Table 7 and Fig. 8 show that almost all of the countries of North and South America belong to one stock-market dominated community, and that the Middle East, Asia and Australia belong to another stock-market dominated community. In contrast, there is one currency community that encompasses the US dollar, a number of Latin American currencies, the Middle East, Russia, India, and several smaller Asian countries, and another currency community that encompasses the Canadian dollar, the Brazilian Real, the Australian dollar, the Euro, and the South African Rand.

We depict the community detection results as an adjacency matrix on the left-hand side and a graphical representation of the networks on the right-hand side of Figs. 9-12. The components, given by  $r_{\alpha\beta}$ , of the adjacency matrix take values between 0 (no synchronization) and 1 (perfect synchronization). The adjacency matrix is visualized using a color code based on a temperature map scheme in which the color changes continuously from blue ( $r_{\alpha\beta} = 0$ ) to red ( $r_{\alpha\beta} = 1$ ) through white ( $r_{\alpha\beta} = 0.5$ ). We give a detailed account of how we obtained the network layouts in Appendix C. The community structure does not change significantly if the network is constructed with a larger or smaller cutoff for the phase differences, e.g.,  $\theta_c/\pi = 0.15$  or  $0.05$  (see Appendix C). However the nature of the communities and the interrelationships between them display different characteristics from period to period.

The visualized adjacency matrices indicate that community C1 increases its synchronization between periods 1 and 3, especially among the European stock markets. This is confirmed by calculating the average correlation coefficients within the communities as shown in Table 8, where we observe an increase from 0.25 in period 1 to 0.57 in period 3. The nodes in C2, consisting mainly of the European currencies, are most tightly coupled in period 2. The average correlation coefficient for C2 increases from 0.58 to 0.72 from period 1 to period 2, and consequently decreases to 0.48 in period 3. Community C3, led by the US dollar, holds approximately the same synchronization strength throughout the entire period with an average correlation coefficient of 0.35. The community C4, dominated by an Asian stock markets

**Table 8: Magnitude of the complex correlation coefficients averaged over all pairs of nodes within each of the four communities, C1, C2, C3, and C4, and across the communities for the entire period (1999-2012) and the three sub-periods, period 1 (1999-2002), period 2 (2003-2006), and period 3 (2007-2012).** These results measure how tightly the communities are synchronized and to what extent residual coupling still remains across the communities.

Community Pair	Entire Period	Period 1	Period 2	Period 3
C1-C1	0.406	0.246	0.307	0.566
C2-C2	0.621	0.576	0.724	0.482
C3-C3	0.265	0.351	0.371	0.347
C4-C4	0.166	0.127	0.101	0.312
C1-C2	0.094	0.005	0.007	0.158
C1-C3	0.053	0.051	0.039	0.051
C1-C4	0.021	0.034	0.024	0.021
C2-C3	0.030	0.017	0.012	0.022
C2-C4	0.003	0.019	0.010	0.000
C3-C4	0.018	0.038	0.016	0.009

group, is well established with an average correlation coefficient increasing from 0.10 in period 2 to 0.31 in period.

Both the adjacency matrices and the network layouts show that C2 is independent in periods 1 and 2 but suddenly changes its characteristics in period 3 when it is strongly connected to C1. On the other hand, C3 is closely related to C1 in the first two periods, and exhibits a stronger connection with C2 in the last period. The independence of community C4 from the rest of the network steadily increases. These findings receive confirmation in the results for the average correlation coefficients across the communities listed in Table 8.

We note that the US stock market and the yen occupy relatively peripheral positions in the financial network throughout the entire period. We also find that the Indian and Korean stock markets do not belong to C4 and remain largely isolated from the main body of the network irrespective of time period.

Table 7 shows how the community structure of the stock and foreign exchange co-moving synchronization network is approximately stable over the entire period and during the three sub-periods, i.e., Period 1, 1999–2002 (mild crisis), Period 2, 2003–2006 (relatively calm), and Period 3, 2007–2012 (severe crisis).

### B. *Temporal relationships between communities*

According to the definition of  $\tilde{C}_{\alpha\beta}$ , the value of  $\theta_{\alpha\beta}$  is the lead phase angle of  $\beta$  against  $\alpha$ . We have already identified four communities arising from the coherent motion of nodes in the equity-currency network. We thus expect that some of them may have a definite lead-lag relation to each other.

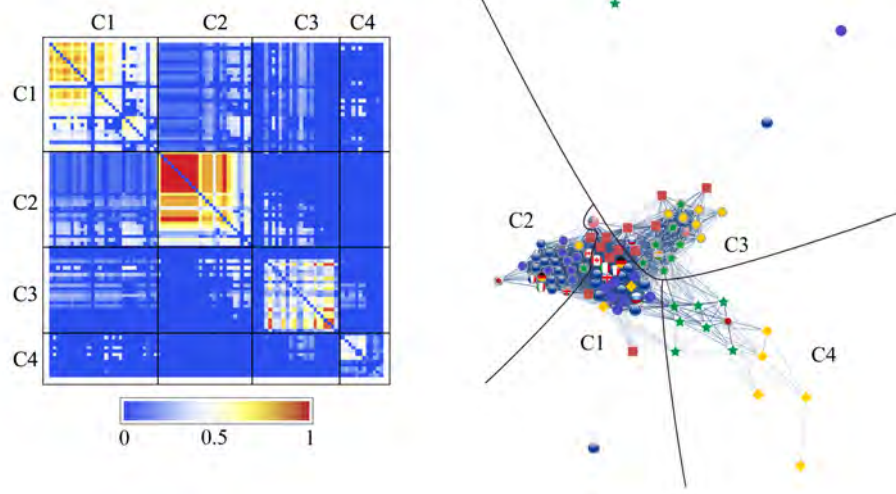


**Figure 9. Community structure for the financial network for the entire period (1999-2012), constructed with  $\theta_c/\pi = 0.1$ .** The left panel shows the adjacency matrix sorted according to the classification into four communities of synchronizing nodes: the 1st community (C1) is a group of stock markets mainly in European and American countries; the 2nd community (C2), a euro-based currency group; the 3rd community (C3), a group of currencies represented by the U.S. dollar; the 4th community (C4), an Asian stock market group surrounding Japan. The right panel shows an optimized layout of the network in an spring-electrical model, with boundaries separating the communities.

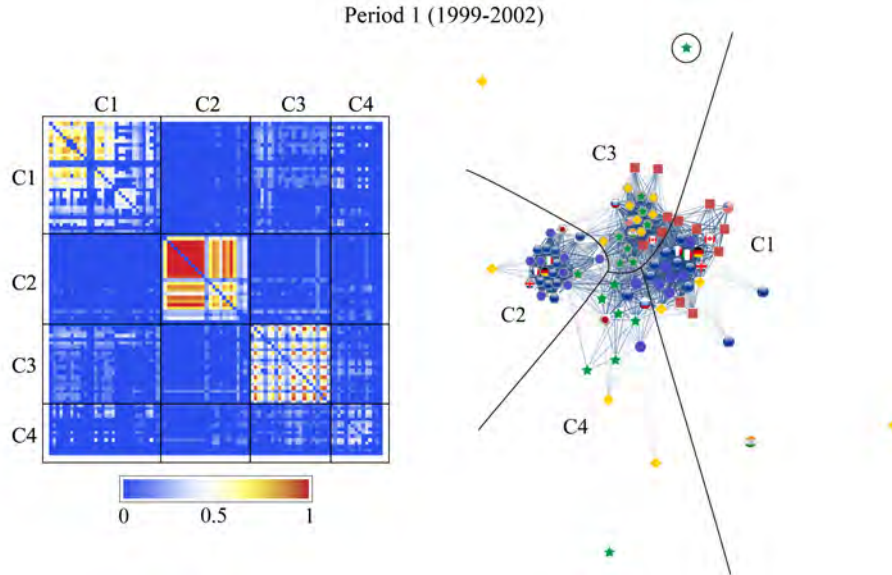


**Figure 10.** Same as Fig. 9, for period 1 (1999-2002). The network consists of four communities as it does in the entire period. The major equity community, C1, has the lowest strength of synchronization in this period while one of the two currency communities, C2, is relatively isolated from the rest of the network; in contrast, the other currency community, C3, is closely related to C1; the Asian equity community C4 is not so strongly connected.

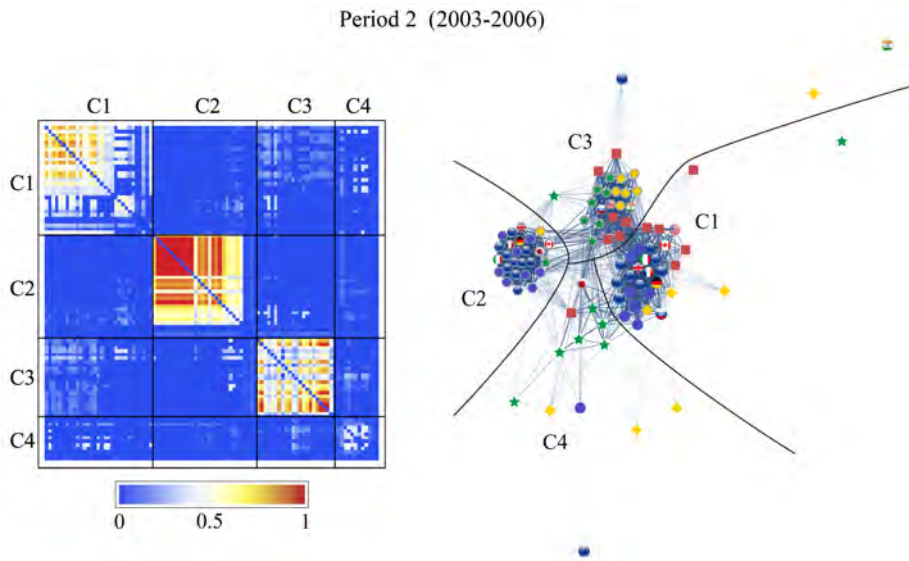


**Figure 11.** Same as Fig. 9, for period 2 (2003-2006). The network is decomposed into four communities to the largest extent in this period; we especially observe that the formation of community C2 is very tight.

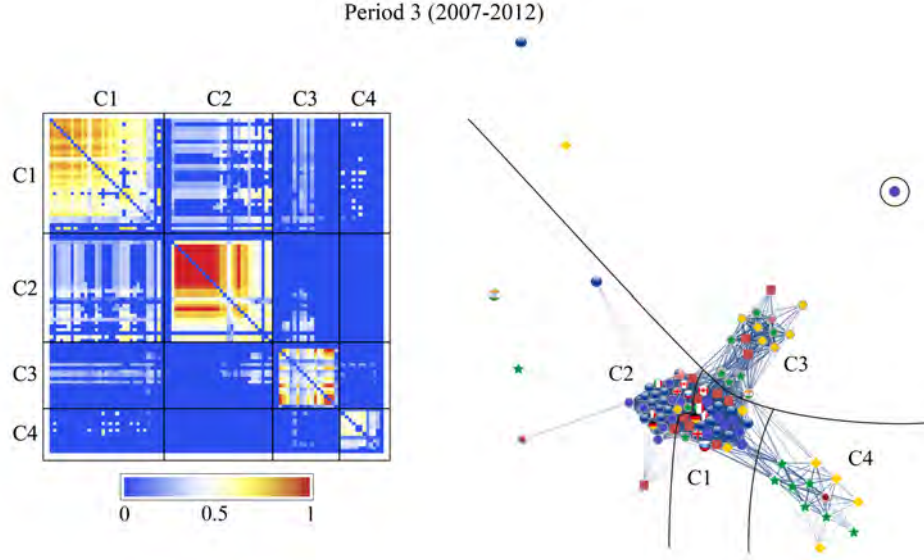


**Figure 12.** Same as Fig. 9, for period 3 (2007-2012). The community structure observed here is quite similar to that obtained in the entire period. This indicates that the global crisis brings a profound influence on the global financial network. Community C1 has the highest degree of synchronization in this period; C2 is now strongly connected to C1 while C3 is further apart from C1 compared to previous sub-periods; C4 has been well established as a group of synchronizing nodes.

Figure 13 shows the correlation coefficients calculated between different communities for the entire period on a complex plane. Note that the distribution of their phases is significantly polarized for every pair of communities. To quantify such a lead-lag relation between  $C_m$  and  $C_n$ , we compute the median for a weighted distribution of the phase differences between the two communities. We define the distribution  $\rho_{mn}(x)$  in terms of Dirac's  $\delta(x)$  as

$$\rho_{mn}(x) = \frac{\sum_{\alpha \in C_m, \beta \in C_n} r_{\alpha\beta} \delta(x - \theta_{\alpha\beta})}{\sum_{\alpha \in C_m, \beta \in C_n} r_{\alpha\beta}}, \quad (26)$$

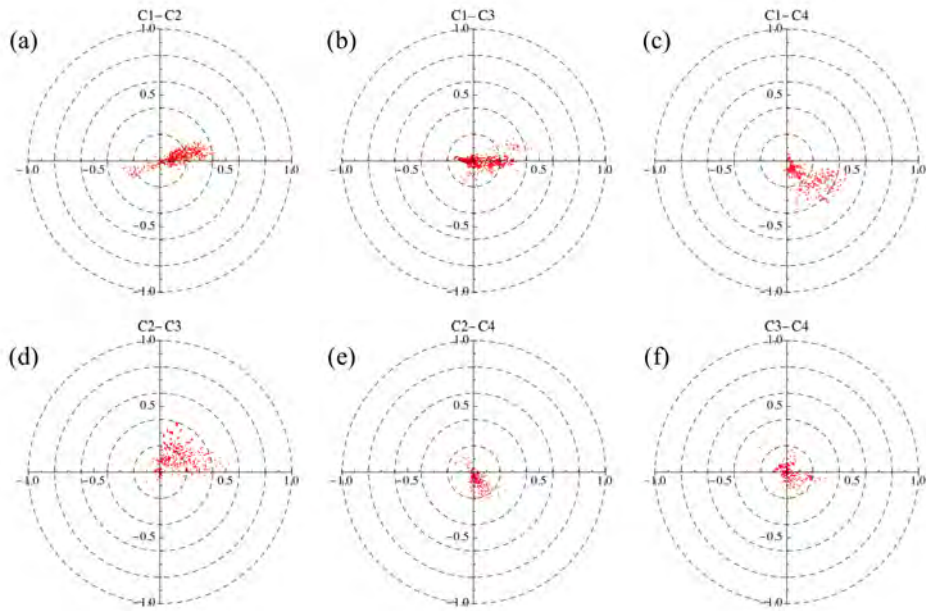
where the correlation strength is understood in terms of weight. The results are 0.053 for C1-C2,  $-0.010$  for C1-C3,  $-0.205$  for C1-C4, 0.276 for C2-C3,  $-0.318$  for C2-C4, and  $-0.045$  for C3-C4 in units of  $1/\pi$ .

Figure 14 shows that community 2 usually leads community 1 which in turn leads community 4, and that community 3 does not have a stable position with respect to the other communities. The distances between communities represent the average phase differences  $\theta_{\alpha\beta}$  weighted by the magnitudes  $r_{\alpha\beta}$ .

We begin by determining the triangular relationship among C1, C2, and C4 by minimizing the geometric discrepancy involved in their phase differences. We set the discrepancy  $D$  as

$$D = (\Theta - \theta_{12})^2 + (\Phi - \theta_{14})^2 + (\Psi - \theta_{24})^2, \quad (27)$$





**Figure 13. Scatter plots of the complex correlation coefficients across the four communities on the complex plane:** (a) for C1-C2, (b) for C1-C3, (c) for C1-C4, (d) for C2-C3, (e) for C2-C4, and (f) for C3-C4. If the correlation coefficients between  $C_m$  and  $C_n$  have a positive median in regards to the distribution of their phases weighted by the associated magnitudes, we infer that  $C_n$  leads  $C_m$ ; if the median is negative, then we infer that  $C_m$  leads  $C_n$

where  $\Theta$ ,  $\Phi$ , and  $\Psi$  are variables corresponding to  $\theta_{12}$ ,  $\theta_{14}$ , and  $\theta_{24}$  to be optimized with constraint  $\Theta - \Phi + \Psi = 0$ . The geometrically consistent phase differences thus obtained are compatible with the original ones with absolute errors of less than  $0.02\pi$  (3.6 degrees). This indicates the three communities are interrelated with a solid causal relation given by  $C2 \rightarrow C1 \rightarrow C4$ . Note that the relation holds over both the entire period and in period 3, i.e., the community structure average for the entire period is very similar to period 3.

Although the C1-C2-C4 triangle is well established, the lead-lag relations determined by the pairs of C1-C3, C2-C3, and C3-C4 give C3 three positions that significantly differ from each other (see Fig. 14). The phase difference between two communities only has meaning on average. This is also the case for the notion of “community of synchronizing nodes.” If the three lead-lag relations indicated in the C1-C3, C2-C3, C3-C4 diagrams are magnified alternatively in time, the multiphase behavior of C3 toward the triangular relationship among C1, C2, and C4 appears.

## V. Conclusion

In this paper we study the interactions between equity and foreign exchange markets for 48 countries between 1999 and 2012. We use insights from statistical physics and network science to model relationships and influences between the foreign exchange

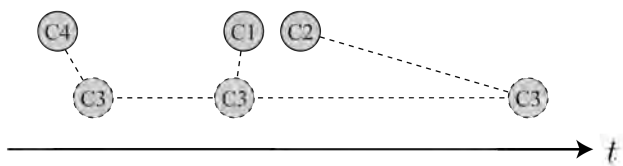


**Figure 14. Lead-lag diagram for the four communities inferred from the results in Fig. 13.** The three communities, C1, C2, and C4, are steadily aligned in the time direction (C2 leading C1 and C4), while C3 has three possible positions depending on which binary correlation is emphasized, C1-C3, C2-C3, or C3-C4.

and stock markets as two interrelated networks that have corresponding nodes and bi-directional dependencies. We use Complex Principal Component Analysis (CPCA) approach to build an interdependent network model for studying the dynamics of this coupled financial system. We construct complex time series by using the Hilbert transformation of the time series for the imaginary component. Using Rotational Random Shuffling (RRS) we find a relatively small number of significant eigenmodes (5 or 6 out of 96 total eigenmodes) and investigate the results obtained by them. We closely examine the eigenvector components corresponding to the three largest eigenvalues of the complex correlation matrix and determine the importance of smaller but significant eigenmodes.

For the entire period between 1999–2012, we observe that in general currency appreciations lead or contribute to positive equity market returns. We also find that the US equity market is an indicator of the future performance of other global stock markets. We also study three distinct sub-periods, the “mild crisis” (1999-2002), “calm” (2003-2006), and “severe crisis” (2007-2012) periods, and find that under different macroeconomic conditions the interactions between the foreign exchange and stock markets vary. We observe that during the mild crisis (1999-2002) sub-period, global equity markets were most able to forecast currency returns. During the calm (2003-2006) sub-period, stock markets exhibited weaker correlations than the foreign exchange markets, which appeared to be more correlated. During the severe crisis (2007-2012) sub-period the interactions between the forex and equity markets were very strong, underlining this period’s strong influence on the overall relationship between currency and stock markets.

We study the intra-relations (within one market) as well as inter-relations (between the two markets) for the forex and equity networks and find distinct clustering in the network that persists for the entire period, which is characterized by behavior that is similar to that in the three distinct sub-periods. We identify four major communities that are approximately stable over time and do not change when the cutoff of the phase differences is changed. The first community (C1) is comprised of equity markets dominated by Europe, the USA, South America, and Canada, the second (C2) of the Canadian dollar and mainly European currencies including the Euro, the third (C3) of the Russian ruble, the US dollar, and selected South American, Asian, and Middle Eastern currencies, and the fourth (C4) of Asian equity

markets, including Japan, and the Middle East. We study the lead-lag relationships between the four communities and find a solid causal relationship for C2 leading C1 and C4, and C1 leading C4, while C3's position in the lead-lag diagram is not settled, but takes three different positions that significantly differ from each another. The network-based approach to model the dynamic structure of equity and foreign exchange markets allows us to capture the topology and interdependence of the two global markets and to find their lead-lag relationships for different macroeconomic environments.

The main contribution of our model is that CPCA combined with RRS offers superior approach for discovering multi-dimensional intrinsic relations within the global financial network of currencies and financial markets. Our approach offers three methodological advantages compared to previous studies: (i) detecting beyond-pairwise lead-lag relationships compared to traditional Granger causality and cross-correlation analysis; (ii) extracting dynamical correlations simultaneously; and (iii) using RRS to provide a sound null hypothesis for identifying statistically significant correlations without making any distribution assumptions of the empirical financial time series that we study.

Another important aspect of our study is the global analysis of “economic regions” rather than “geographical regions.” These economic regions we can see emerge according to the composition of our network communities. For example, American stock markets belong to the same community (C1), but American currencies belong to the same community (C3) as Asian currencies. The Japanese Yen does not belong to the community dominated by Asian currencies but to the community dominated by European currencies (C2), where we also find the Australian Dollar and the South African Rand. Thus we can emphasize that an “economic region” is in fact quite different from a “geographic region” and that studies limited to geographic regions will not detect the interrelationships among truly global financial and economic trends.

This model could be expanded beyond our study of the interdependencies between the foreign exchange market and the stock market to include global fixed income, credit default swaps, interest rates, options, futures, and other financial markets and instruments. We suggest that this methodology could be useful in the development of a tool for real-time monitoring of the dynamics of global financial markets, one that could enable policy makers and regulators to daily monitor systemic risk fluctuations in the global financial system.

### A. Detailed study of the CPCA eigensystem for each period

In this appendix, we give the detailed account of the CPCA eigenvalues and eigenvectors for each of the three periods.

The comparisons of the eigenvalues and the RRS eigenvalue distribution are given in Fig.A1 for periods 1, 2 and 3 from top to the bottom in the manner of Fig.1. From these, we learn that top 5 eigenvalues for periods 1 and 2, and top 6 eigenvalues for period 3 are clearly outside of the range of the RRS distribution and are significant.

These eigenvectors of the three periods may be decomposed in terms of the eigenvectors for the whole period as follows:

$$\mathbf{V}_p^{(n)} = \sum_{m=1}^N c_p^{(n,m)} \mathbf{V}^{(m)}, \quad (\text{A1})$$

where  $\mathbf{V}_p^{(n)}$  is the  $n$ -th eigenvector for the period  $p$  ( $= 1, 2, 3$ ). Since  $\mathbf{V}$  and  $\mathbf{V}_p$ 's

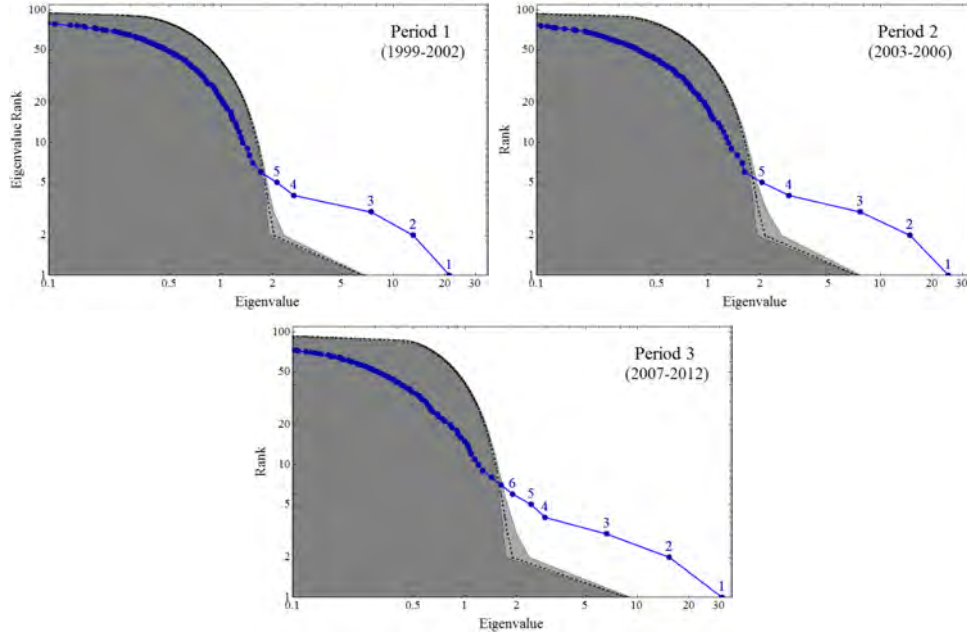


**Figure A1. Significant eigenvalues identified by the CPCA with RRS results for periods 1-3.** The blue dot denoted ' $n$ ' shows the  $n$ -th largest CPCA eigenvalue ( $x$ -axis) and the CPCA eigenvalue rank ( $y$ -axis). The gray small dots and the lighter gray area show the average RRS and the 99% range. The largest 5 eigenvalues in periods 1 and 2, and the largest 6 eigenvalues for period 3 are clearly outside of each of their RRS ranges. and show significant relationships in the interdependent network.

span complete set, the decomposition coefficients  $c_p^{(n,m)}$  satisfies

$$\sum_{m=1}^N \left| c_p^{(n,m)} \right|^2 = 1. \quad (\text{A2})$$

The coefficients  $\left| c_p^{(n,m)} \right|^2$  are given in Fig. A2, with  $m$  on the x-axis and  $n$  in descending order from top to bottom in each plot (denoted as “No. $n$ ”). We observe the following in these plots:

1. Top 5 (for periods 1 and 2) and 6 (for period 3) eigenvectors are well-approximated by linear-combinations of the top 6 (significant) eigenvectors of the whole period. This confirms that 6 significant eigenmodes of the whole period are sufficient for looking into specific periods, validating mode-signal analysis by the top 6 eigenmodes, described in Appendix B.
2. Among all three periods, the eigenvector structure of period 3 most similar to the structure of the entire period: In the period 3, No.1 eigenvector is mostly represented by the top eigenvector of the entire period, No.2 and No.3 are mixtures of the second and the third eigenvectors of the entire period, while No. 4, 5, and 6 are mostly based on their corresponding counterpart of the entire period. This confirms the fact that period 3, representing the severe crisis period and exhibiting significant co-motion within the synchronization network, dominates the entire period and plays essential part in the determination of the eigenmodes of the entire period.

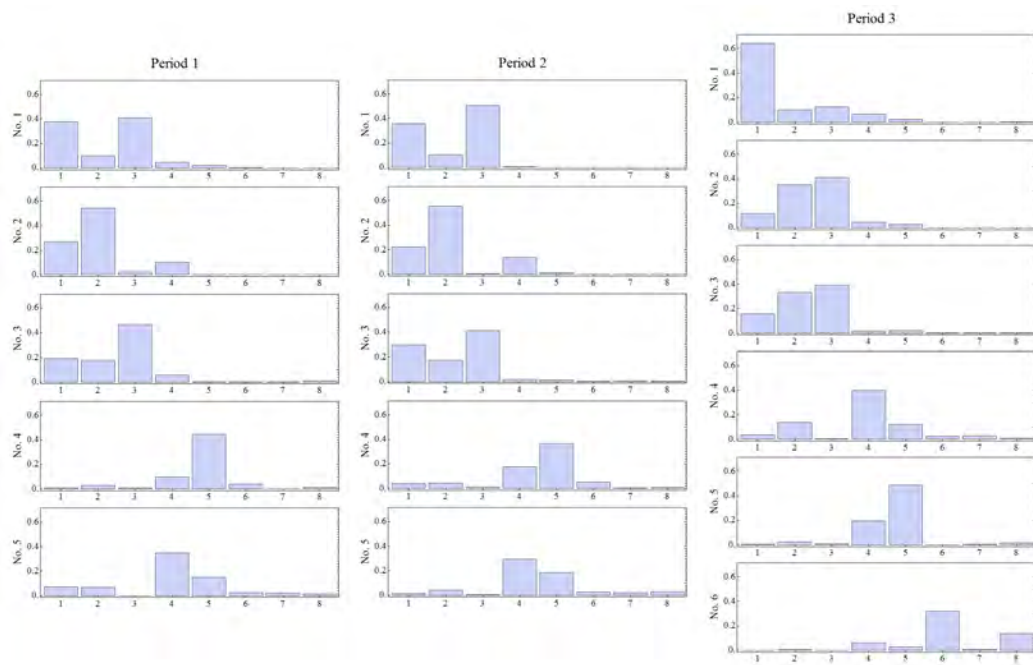


Figure A2. Decomposition of the eigenvectors in each period in terms of eigenvectors of the entire period.

## B. Visualization of Significant and Complexified Time-series

In our analysis of complex correlation matrix, the complexified time-series are expanded in terms of the eigenvectors for the complex correlation matrix, namely in the expansion given by Eq. (15). We found by the RRS method that the number of significant eigenvalues and corresponding eigenvectors can be estimated to be 6 for the entire period.

We are able to select those first  $N_s = 6$  significant terms in the full expansion of  $N$  terms:

$$\tilde{w}_\alpha^{(N_s)}(t) := \sum_{n=1}^{N_s} a^{(n)}(t) \mathbf{V}_\alpha^{(n)}, \quad (\text{B1})$$

regarding the other terms as “noise”. Fig. B1 depicts the absolute values of  $a^{(n)}(t)$  for  $n = 1, 2, \dots, N_s = 6$  (from top to bottom) during the entire period of time.

One can observe that on average, the first mode-signal corresponding to the largest eigenvalue dominates over the other mode-signals. Recall the relation Eq. (16) which states that the *average* of  $a^{(1)}$  is greater than that of  $a^{(n)}$  for  $n > 1$ , because  $\lambda^{(1)} > \lambda^{(n)}$ . The plots in Fig. B1 show that the first mode-signal dominates the others, not only in an averaged sense but also for almost all time. Similar observation holds for the other mode-signals in decreasing order of  $n$ . The striking exception is the  $n = 6$  mode-signal, which becomes as strong as the  $n = 1$  at the time of the Lehman Brothers crisis, as discussed in subsection IIB.

We can further convert from  $\tilde{w}_\alpha(t)$  to  $\tilde{r}_\alpha(t)$  by using Eq. (8) in the opposite way:

$$\tilde{r}_\alpha^{(N_s)}(t) := \langle \tilde{r}_\alpha \rangle_t + \sigma_\alpha \cdot \tilde{w}_\alpha^{(N_s)}(t) \quad (\text{B2})$$

so that we can construct the significant and complexified time-series by using those 6 mode-signals and corresponding eigenvectors.

The resulting time-series  $\tilde{r}_\alpha^{(N_s)}(t)$  are significant co-movements that can be visualized by a set of points, equities or currencies of  $\alpha$ , on the complex plane at each point of time  $t$ . We provide as a supplementary material a visualization for the movements of those points from January 1999 to December 2012. Users can manipulate the visualized co-movements of equities and currencies along the time-line to see how significant co-movements change at epochs; mild crisis, calm period, severe crisis, and particular dates of interest. See our web page in Vodenska et al. (2014).

How the points of equities and currencies are dispersed on the complex plane can be quantified by a measure of dispersion at each time  $t$ :

$$D(t) := \sqrt{\sum_{\alpha} |\tilde{r}_\alpha^{(N_s)}(t)|^2} \quad (\text{B3})$$

The temporal change of  $D(t)$  is shown in Fig. B2. We can observe many bursts of  $D(t)$  at different times, which signal significant changes at the respective periods. If, in addition, a set of points in the complex plane has a radial line-up, such a set of points implies a significant co-movements. It should be noted in Fig. B2 that

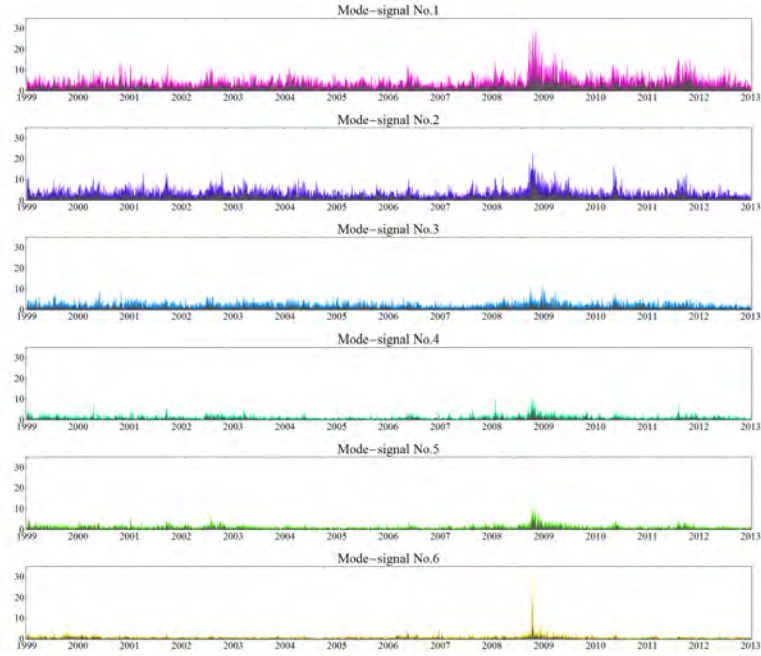


**Figure B1. Absolute values of the mode-signals  $a^{(n)}(t)$  for  $n = 1, 2, \dots, N_s = 6$  during the entire period of time.** Mode-signal  $a^{(n)}$  dominates the others  $a^{(m)}$  for  $m > n$ , not only in the average sense (as expected from the relation in Eq. (16), that is satisfied by the mode-signals), but also for all the periods. A striking exception is the  $n = 6$  mode-signal, which becomes as strong as the first,  $n = 1$ , mode-signal at the time of the Lehman Brothers crisis. See also subsection IIB.

the most striking dispersion occurs during the Lehman Brothers crisis in the third quarter of 2008, which brought about a subsequent volatile period continuing into the European sovereign debt crisis that followed.



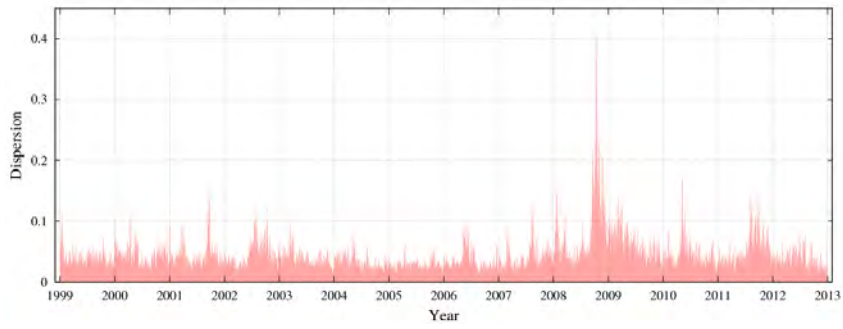


**Figure B2.** Dispersion  $D(t)$  of the equities and currencies, defined by Eq. (B3), calculated from the significant and complexified time-series,  $\tilde{r}_\alpha^{(N_s)}(t)$ . We observe many bursts with significant signal changes at different time periods. If, in addition to the dispersion, a set of points in the complex plane has a radial line-up, this implies significant co-movements. The most striking dispersion corresponds to the Lehman Brothers crisis in the third quarter of 2008 followed by a subsequent volatile period corresponding to the European sovereign debt crisis.

### C. Methodology used to detect network communities

We identify community structures of the financial networks by maximizing a quality function known as modularity (Newman and Girvan (2004)). This is a prevailing method to detect communities in complex networks (Fortunato (2010)). The modularity  $Q$  for an unweighted network with  $M$  links which is decomposed into  $L$  communities is defined as

$$Q = \sum_{s=1}^L \left[ \frac{e_s}{M} - \left( \frac{d_s}{2M} \right)^2 \right], \quad (\text{C1})$$

where  $e_s$  and  $d_s$  are the total number of internal links and the sum of degree of nodes within community  $s$ , respectively. The value of  $L$  is also simultaneously determined through the modularity maximization. The modularity measures the fraction of links within the given communities of a network in reference to the expected fraction of the intralinks if the network is randomized with the degree of each node preserved. For the modularity of weighted networks such as those studied here, one may generalize Eq. (C1) by replacing the unit weight of each link by its actual weight (Newman (2004)); for instance, the degree of each node is the total sum of weights of its connecting links. To carry out maximization of the modularity, in fact, we adopted the fast unfolding method (Blondel et al. (2008)). Since this is a computational method of stochastic nature, we repeat the procedure using different series of random numbers to obtain 10,000 partitions and select the result with the largest modularity.

Visualization is another useful tool to illuminate structural properties of complex networks. To have an optimized layout for each of our networks, we adopt a spring-electrical model in which pairs of nodes with direct links are physically connected with springs and any pairs of nodes repel each other through a repulsive Coulomb force (Hu (2006)). The attractive force due to the spring keeps tightly connected nodes close in a space. On the other hand, the repulsive Coulomb force tends to distribute nodes uniformly over the available space and to prevent entanglement of the network. The optimization for the network layouts were then obtained by gradually cooling "temperature" of the fictitious system to zero temperature through molecular dynamics simulations (Frenkel and Smit 2002).

The choice of the cutoff angle  $\theta_c$  to determine synchronizing nodes (markets and currencies) needs careful study. Here we demonstrate to what extent the community structure depends on  $\theta_c$  in Figs. C1 and C2 corresponding to Fig. 9 for the entire period, where the cutoff value one and a half times or half as large as that in Fig. 9 is adopted. The number of links drops from 4,644 for  $\theta_c/\pi = 0.15$  to 3,890 for  $\theta_c/\pi = 0.1$  and to 2,616 for  $\theta_c/\pi = 0.05$ . We see that the four community structure as has been already identified is stable against such substantial change of  $\theta_c$ . This is also true for all of the results obtained with the varied cutoffs in the three partial periods with two exceptions. In periods 1 and 2, the two stock market communities are combined into one group at the largest value of  $\theta_c$ . However, one can easily identify the two sub-communities in the combined community. Therefore, we infer

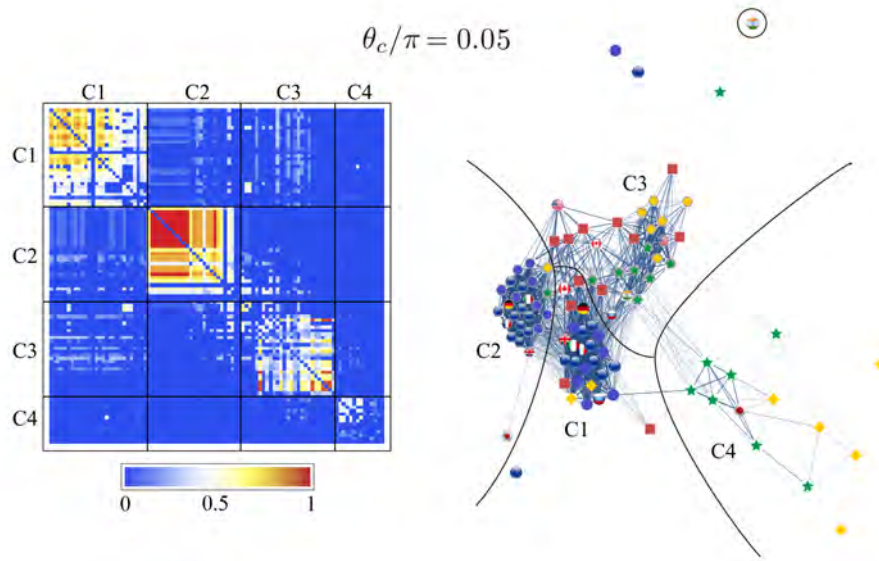


**Figure C1. Community structure for  $\theta_c = 0.05$ .** Lowering  $\theta_c$  by half decreases the number of links from 3,890 to 2,616 and hence makes the network considerably sparser. However, the four community structure resembling to that in Fig. 9 still survives.

that the construction of the synchronization network and its community structure is robust with respect to the choice of the cutoff value  $\theta_c$ .

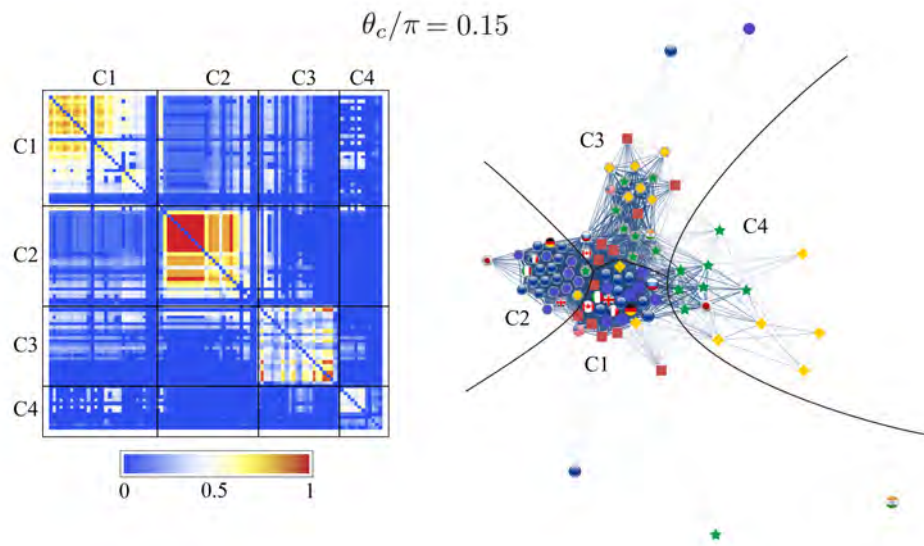


**Figure C2. Community structure for  $\theta_c = 0.15$ .** Raising  $\theta_c$  by one and a half increases the number of links from 3,890 to 4,644, leading to a network in which nodes are more tightly connected. However, we still observe four communities organized in almost the same way as in Fig. 9.

## References

- Acemoglu, Daron, Vasco M Carvalho, Asuman Ozdaglar, and Alireza Tahbaz-Salehi, 2012, The network origins of aggregate fluctuations, *Econometrica* 80, 1977–2016.
- Acemoglu, Daron, Asuman Ozdaglar, and Alireza Tahbaz-Salehi, 2013, Systemic risk and stability in financial networks, Technical report, National Bureau of Economic Research.
- Ang, Andrew, and Geert Bekaert, 2007, Stock return predictability: Is it there?, *Review of Financial Studies* 20, 651–707.
- Aoyama, Hideaki, Stefano Battiston, and Yoshi Fujiwara, 2013, Debtrank analysis of the Japanese credit network, *RIETI Discussion Papers* 13-E-087, 1–19.
- Arai, Y., and H. Iyetomi, 2013, Complex principal component analysis of dynamic correlations in financial markets, *Intelligent Decision Technologies, Frontiers in Artificial Intelligence and Applications* 255, 111–119.
- Bae, Kee-Hong, G Andrew Karolyi, and Rene M Stulz, 2003, A new approach to measuring financial contagion, *Review of Financial studies* 16, 717–763.
- Battiston, Stefano, Domenico Delli Gatti, Mauro Gallegati, Bruce Greenwald, and Joseph E Stiglitz, 2012, Liaisons dangereuses: Increasing connectivity, risk sharing, and systemic risk, *Journal of Economic Dynamics and Control* 36, 1121–1141.
- Bekaert, Geert, and Robert J Hodrick, 1992, Characterizing predictable components in excess returns on equity and foreign exchange markets, *The Journal of Finance* 47, 467–509.
- Bekaert, Geert, Robert J Hodrick, and Xiaoyan Zhang, 2009, International stock return comovements, *The Journal of Finance* 64, 2591–2626.
- Billio, Monica, Mila Getmansky, Andrew W Lo, and Lioriana Pelizzon, 2010, Econometric measures of systemic risk in the finance and insurance sectors, Technical report, National Bureau of Economic Research.
- Blondel, Vincent D, Jean-Loup Guillaume, Renaud Lambiotte, and Etienne Lefebvre, 2008, Fast unfolding of communities in large networks, *Journal of Statistical Mechanics: Theory and Experiment* 2008, P10008.
- Bollerslev, Tim, James Marrone, Lai Xu, and Hao Zhou, 2012, Stock return predictability and variance risk premia: statistical inference and international evidence, *Available at SSRN 2023552* .
- Breen, William, Lawrence R Glosten, and Ravi Jagannathan, 1989, Economic significance of predictable variations in stock index returns, *The Journal of Finance* 44, 1177–1189.

- Buldyrev, Sergey V, Nathaniel W Shere, and Gabriel A Cwilich, 2011, Interdependent networks with identical degrees of mutually dependent nodes, *Physical Review E* 83, 016112.
- Cappiello, Lorenzo, and Roberto A De Santis, 2005, *Explaining exchange rate dynamics: The uncovered equity return parity condition* (Citeseer).
- Cochrane, John H, 2008, The dog that did not bark: A defense of return predictability, *Review of Financial Studies* 21, 1533–1575.
- Cohen, Lauren, and Andrea Frazzini, 2008, Economic links and predictable returns, *The Journal of Finance* 63, 1977–2011.
- Dahlquist, Magnus, and Henrik Hasseltoft, 2013, International bond risk premia, *Journal of International Economics* 90, 17–32.
- Dehmamy, Nima, Sergey V Buldyrev, Shlomo Havlin, H Eugene Stanley, and Irena Vodenska, 2014, A systemic stress test model in bank-asset networks, *arXiv preprint arXiv:1410.0104* .
- Dooley, Michael, and Peter Isard, 1982, A portfolio-balance rational-expectations model of the dollar-mark exchange rate, *Journal of International Economics* 12, 257–276.
- Dornbusch, Rudiger, and Stanley Fischer, 1980, Exchange rates and the current account, *The American Economic Review* 70, 960–971.
- Fama, Eugene F, and Kenneth R French, 1988, Dividend yields and expected stock returns, *Journal of Financial Economics* 22, 3–25.
- Fama, Eugene F, and Kenneth R French, 1989, Business conditions and expected returns on stocks and bonds, *Journal of Financial Economics* 25, 23–49.
- Ferreira, Miguel A, and Pedro Santa-Clara, 2011, Forecasting stock market returns: The sum of the parts is more than the whole, *Journal of Financial Economics* 100, 514–537.
- Ferson, Wayne E, and Campbell R Harvey, 1993, The risk and predictability of international equity returns, *Review of Financial Studies* 6, 527–566.
- Fortunato, Santo, 2010, Community detection in graphs, *Physics Reports* 486, 75–174.
- Frenkel, Daan, and Berend Smit, 2002, *Understanding Molecular Simulation: From Algorithms to Applications*, second edition (Academic Press, San Diego).
- Gagnon, Louis, and G Andrew Karolyi, 2006, Price and volatility transmission across borders, *Financial Markets, Institutions & Instruments* 15, 107–158.

- Gai, Prasanna, Andrew Haldane, and Sujit Kapadia, 2011, Complexity, concentration and contagion, *Journal of Monetary Economics* 58, 453–470.
- Gao, Jianxi, Sergey V Buldyrev, H Eugene Stanley, and Shlomo Havlin, 2011, Networks formed from interdependent networks, *Nature Physics* 8, 40–48.
- Granger, Clive WJ, Bwo-Nung Huangb, and Chin-Wei Yang, 2000, A bivariate causality between stock prices and exchange rates: evidence from recent asian-flu, *The Quarterly Review of Economics and Finance* 40, 337–354.
- Haldane, Andrew G, and Robert M May, 2011, Systemic risk in banking ecosystems, *Nature* 469, 351–355.
- Harvey, Campbell R, 1991, The world price of covariance risk, *The Journal of Finance* 46, 111–157.
- Hjalmarsson, Erik, 2010, Predicting global stock returns .
- Hong, Harrison, Walter Torous, and Rossen Valkanov, 2007, Do industries lead stock markets?, *Journal of Financial Economics* 83, 367–396.
- Huang, Xuqing, Irena Vodenska, Shlomo Havlin, and H Eugene Stanley, 2013, Cascading failures in bi-partite graphs: Model for systemic risk propagation, *Scientific Reports* 3.
- Huang, Xuqing, Irena Vodenska, Fengzhong Wang, Shlomo Havlin, and H Eugene Stanley, 2011, Identifying influential directors in the united states corporate governance network, *Physical Review E* 84, 046101.
- Iyetomi, Hiroshi, Yasuhiro Nakayama, Hiroshi Yoshikawa, Hideaki Aoyama, Yoshi Fujiwara, Yuichi Ikeda, and Wataru Souma, 2011, What causes business cycles? analysis of the japanese industrial production data, *Journal of the Japanese and International Economies* 25, 246–272.
- Katechos, Georgios, 2011, On the relationship between exchange rates and equity returns: A new approach, *Journal of International Financial Markets, Institutions and Money* 21, 550–559.
- Lin, Chien-Hsiu, 2012, The comovement between exchange rates and stock prices in the asian emerging markets, *International Review of Economics & Finance* 22, 161–172.
- Majdandzic, Antonio, Lidia A Braunstein, Chester Curme, Irena Vodenska, Sary Levy-Carciente, H Eugene Stanley, and Shlomo Havlin, 2015, Multiple tipping points and optimal repairing in interacting networks, *arXiv preprint arXiv:1502.00244* .
- Marčenko, V. A., and L. A. Pastur, 1967, Distribution of eigenvalues for some sets of random matrices, *Mathematics of the USSR-Sbornik* 1, 457–483.

- Menzly, Lior, and Oguzhan Ozbas, 2010, Market segmentation and cross-predictability of returns, *The Journal of Finance* 65, 1555–1580.
- Morley, Bruce, 2002, Exchange rates and stock prices: implications for european convergence, *Journal of Policy Modeling* 24, 523–526.
- Newman, Mark EJ, 2004, Analysis of weighted networks, *Physical Review E* 70, 056131.
- Newman, Mark EJ, and Michelle Girvan, 2004, Finding and evaluating community structure in networks, *Physical Review E* 69, 026113.
- Nieh, Chien-Chung, and Cheng-Few Lee, 2002, Dynamic relationship between stock prices and exchange rates for g-7 countries, *The Quarterly Review of Economics and Finance* 41, 477–490.
- Ning, Cathy, 2010, Dependence structure between the equity market and the foreign exchange market—a copula approach, *Journal of International Money and Finance* 29, 743–759.
- Pan, Ming-Shiun, Robert Chi-Wing Fok, and Y Angela Liu, 2007, Dynamic linkages between exchange rates and stock prices: Evidence from east asian markets, *International Review of Economics & Finance* 16, 503–520.
- Patro, Dilip K, and Yangru Wu, 2004, Predictability of short-horizon returns in international equity markets, *Journal of Empirical Finance* 11, 553–584.
- Rapach, David E, Jack K Strauss, and Guofu Zhou, 2013, International stock return predictability: what is the role of the united states?, *The Journal of Finance* 68, 1633–1662.
- Rapach, David E, and Mark E Wohar, 2006, In-sample vs. out-of-sample tests of stock return predictability in the context of data mining, *Journal of Empirical Finance* 13, 231–247.
- The Economist, 2008, Cracks in the crust, *The Economist* <http://www.economist.com/node/12762027>.
- Vodenska, I., H. Aoyama, Y. Fujiwara, Y. Iyetomi, and Y. Arai, 2014, Supplementary information, [http://www.econophysics.jp/download/vodenska\\_et\\_al\\_2014/index.html](http://www.econophysics.jp/download/vodenska_et_al_2014/index.html).
- Welch, Ivo, and Amit Goyal, 2008, A comprehensive look at the empirical performance of equity premium prediction, *Review of Financial Studies* 21, 1455–1508.
- Zhao, Hua, 2010, Dynamic relationship between exchange rate and stock price: Evidence from china, *Research in International Business and Finance* 24, 103–112.